National Library of Canada

Acquisitions and Bibliographic Services Branch

395 Wellington Street
Ottawa, Ontario
K1A 0N4

Bibliothèque nationale du Canada

Direction des acquisitions et des services bibliographiques

395, rue Wellington
Ottawa (Ontario)
K1A 0N4

Your file Votre référence

Our file Notre référence

NOTICE

The quality of this microform is heavily dependent upon the quality of the original thesis submitted for microfilming. Every effort has been made to ensure the highest quality of reproduction possible.

If pages are missing, contact the university which granted the degree.

Some pages may have indistinct print especially if the original pages were typed with a poor typewriter ribbon or if the university sent us an inferior photocopy.

Reproduction in full or in part of this microform is governed by the Canadian Copyright Act, R.S.C. 1970, c. C-30, and subsequent amendments.

AVIS

La qualité de cette microforme dépend grandement de la qualité de la thèse soumise au microfilmage. Nous avons tout fait pour assurer une qualité supérieure de reproduction.

S'il manque des pages, veuillez communiquer avec l'université qui a conféré le grade.

La qualité d'impression de certaines pages peut laisser à désirer, surtout si les pages originales ont été dactylographiées à l'aide d'un ruban usé ou si l'université nous a fait parvenir une photocopie de qualité inférieure.

La reproduction, même partielle, de cette microforme est soumise à la Loi canadienne sur le droit d'auteur, SRC 1970, c. C-30, et ses amendements subséquents.

Canada

AN ELECTROCHEMICAL QUARTZ CRYSTAL MICROBALANCE STUDY OF ADSORPTION PROCESSES AT GOLD ELECTRODES

Tao Ding

ISBN 0-315-82531-6

Canada

UNIVERSITÉ D'OTTAWA
UNIVERSITY OF OTTAWA

To the Memory of My

Grandmother

&

Mother

Acknowledgments

I would like to express my deepest and sincere thanks to my supervisor, Dr. C.P.Wilde, for his direction, guidance, patience and creative input throughout the course of this work. He not only gave me assistance in research but also helped me with my English. Without his help, it would have been impossible to complete this work.

I am grateful to my colleague, M. Zhang, who discussed problems with me and helped me set up the equipment.

I would like to express my gratitude to glassblowers, Mr. E. Kristoff and Mr. J. Hopkins who made the glass cells; to electrician Mr. F. Allard who made the electronic circuits and machinist Mr. D. Hopkins for his help with mechanics.

I also would like to thank all members of the chemistry office for their administrative assistance.

A very special thanks to my husband for all the help and support.

Finally, I am thankful to my father and all members of my family for their love and attitudes to me all the time.

Abstract

This thesis describes a study of the adsorption of anions and neutral organic molecules at gold electrodes using the electrochemical quartz crystal microbalance (EQCM). Differential capacitance, cyclic voltammetry and ring-disk methods were also used to provide further data.

In perchlorate solutions (except 0.1 M $HClO_4$) mass responses are flat at potentials positive of the potential of zero charge (E_{pzc}) in the double layer region of potential. This seems to agree with the accepted view that perchlorate adsorbs weakly at gold. When phosphate is added to 0.1 M $KClO_4$ the mass response is seen to increase with increasing potential positive of the E_{pzc}. The size of this increase is proportional to the concentration of phosphate species. Differential capacitance and cyclic voltammetry data confirm the adsorption of phosphate species.

Adsorption of 4,4'-bipyridyl was studied because it is one of many compounds that, when adsorbed, promote the electrochemistry of cytochrome c. The presence of 4,4'-bipyridyl at the electrode surface removes the mass change seen in phosphate buffer and produces a flat mass change over the potential range from -0.6 V to 0.6 V. Replacement of adsorbed ions is confirmed by differential capacitance experiments. When the electrode surface is oxidised in the presence of 4,4'-bipyridyl, no significant mass increase is observed. The mass response also shows that reversal of the place exchange process

(where an O species is inserted into the gold lattice upon oxidation) leads to removal of a small amount of adsorbate and an irreversible loss of material from the electrode. A possible mechanism has been proposed which would account for these observations. Finally, EQCM responses show clearly that adsorbed bipyridyl is easily removed from the electrode surface by washing.

Claims to Original Research

1. Strongly adsorbing anions (HPO_4^{2-}, $H_2PO_4^-$) have been shown to influence the mass response of a gold electrode in the double layer region of potential.
2. The replacement of strongly adsorbing anions by 4,4'-bipyridyl has been demonstrated by observation of changes in the EQCM response.
3. The reversal of the place exchange process upon electrode surface reduction has been shown to displace adsorbed 4,4'-bipyridyl.
4. Two unusual effects have been observed. The first is the increase in mass observed at potentials below the E_{pzc}. The second is the isomass point. These effects require further work before they can be explained.

One paper, describing some of the work reported here, has been published.

- C. P. Wilde and T. Ding, J. Electroanal. Chem., 327 (1992) 279.

List of Figures

Figure 30. Current-potential curves in 0.1 M phosphate buffer at a gold ring-gold disc electrode. ω = 25 Hz, Scan rate = 50 mV/s.

Figure 31. Cyclic voltammogram for an EQCM gold electrode in 0.1 M $KClO_4$/0.02 M phosphate solution with no Bipy (upper curve) and after adsorption of 0.5 mM 4,4'-bipyridyl for 30 minutes at open circuit (lower curve). Scan rate = 20 mV/s. The lower curve was recorded in the electrolyte containing 0.5 mM Bipy.

Figure 32. Differential capacitance-potential curves of the EQCM gold electrode in 0.1 M $KClO_4$/0.02 M phosphate solution containing (a) 0, (b) 0.1 mM, (c) 0.5 mM 4,4'-bipyridyl. Scan rate = 20 mV/s. Frequency = 16 Hz.

Figure 33. Mass responses for an EQCM gold electrode in 0.1 M $KClO_4$/0.02 M phosphate buffer with no Bipy (upper curve) and after adsorption of 5 mM 4,4'-bipyridyl for 30 minutes at open circuit (lower curve). Scan rate = 20 mV/s. The lower curve was recorded in the electrolyte containing 5 mM Bipy.

Figure 34. Two orientations of 4,4'-bipyridyl adsorption at gold electrode surface. (A) parallel, (B) vertical.

Figure 35. Typical cyclic voltammogram (top) , and the mass responses that accompany the first (lowest), third (middle) and fifth (upper) voltammograms after replacement of a 5 mM Bipy containing electrolyte with fresh phosphate buffer. Scan rate = 20 mV/s. The mass responses are displaced along the

vertical axis for clarity.

Figure 36. Cyclic voltammogram and mass response for gold electrode after immersion in an electrolyte containing 5 mM Bipy for 1 hour (at open circuit). Response recorded with 5 mM Bipy still in the electrolyte at a scan of 20 mV/s.

Figure 37. Cyclic voltammogram and mass responses for a gold electrode after being exposed to a 5 mM solution of Bipy overnight. The anodic potential limit was taken to successively more positive potentials for 8 cycles. Some cycles are omitted for clarity. Mass responses are offset from each other for the same reason and results were obtained with 5 mM Bipy remaining in the electrolyte. Scan rate = 20 mV/s.

Figure 38. Cyclic voltammogram (first scan only) and mass response for gold electrode such as that of Figure 36, after replacement of 4,4'-bipyridyl containing electrolyte with fresh phosphate buffer. Solid line - Mass response accompanying the first scan, dashed line accompanying second scan.

TABLE OF CONTENTS

Chapter 1: Introduction

Chapter 2: Experimental

Chapter 3: Literature Review

Adsorption of Bipyridyl Molecules at Different Metal Electrodes

Chapter 4: Results and Discussion

Chapter 1: INTRODUCTION

This thesis is concerned with the use of the Electrochemical Quartz Crystal Microbalance in the study of adsorption processes at electrodes. Electrochemical methods such as differential capacitance were also used for the same purpose. This chapter presents an introduction to both methods as well as a description of the structure of the electrode/solution interface.

1.1. Electrochemical Quartz Crystal Microbalance

The electrochemical quartz crystal microbalance (EQCM) is an extension of the quartz crystal microbalance (QCM), which allows the in-situ measurement of mass changes occurring at the surfaces of electrodes. This is achieved through the use of electrodes deposited onto oscillating quartz wafers and the recording of the frequency of oscillation together with the electrochemical response. Under appropriate circumstances, mass changes of the order of 10^{-9} g can be measured.

The quartz crystal microbalance has had broad utilization as a mass sensor in applied physics, chemistry, surface science and many other areas of technology[1] because of its sensitivity and simplicity. Examples of the use of QCM's include the detection and determination of various air pollutants (sulphur dioxide, hydrogen sulphide, hydrogen

chloride, organo-phosphorus compounds, pesticides, aromatic hydrocarbons, mercury, mononitrotoluene and carbon monoxide), simultaneous measurement of mass and temperature, and studies of space system contamination etc[1]. More recently, the QCM has been demonstrated to be very useful for measuring mass changes in the nanogram range occurring during in-situ electrochemical experiments[2 - 6].

In this chapter the physical origin of mass sensing will be presented as it was described originally by Sauerbrey[7] for sensing applications in the gas phase. The extension of the QCM to applications in solution will then be outlined.

1.1.1. The Physical Origin of Mass Sensing

i) Piezoelectric Effect

When pressure is applied to a small piece of some crystals in a particular direction, an electrical potential is produced between deformed surfaces, this potential being proportional to the applied pressure. This is the piezoelectric (derived from Greek: "piezin" meaning to press) or the "pressure electric" effect. This feature only exists in acentric materials (called piezoelectric materials). A single crystal of piezoelectric material has dipoles associated with the orientation of atoms in the crystalline lattice and so it has a polar axis. As a piezoelectric material, the quartz wafer becomes slightly deformed in the presence of an electric field because the resulting atomic displacement

will produce a corresponding change in the net dipole moment if a stress is applied in an appropriate direction. This deformation will generate a net change in the electrical charge on the faces of the crystal (Figure 1). Microbalances make use of the converse piezoelectric effect where application of a voltage to a crystal gives rise to a corresponding mechanical strain.

ii) Quartz Crystal Resonator

A piezoelectric quartz crystal resonator is a precisely cut slice from a natural or synthetic single crystal of quartz. The application of an external varying electric potential to a piezoelectric material produces mechanical oscillations within the crystal lattice, whereas a constant potential will cause a deformation of the crystal. When used in the QCM, the quartz wafer is sandwiched between two electrodes attached to the wafer surface (Figure 2). Thus, when electrodes are affixed to a quartz crystal wafer and connected to a periodic voltage source, the quartz crystal unit may be made to vibrate at the frequency of the driving voltage. If the frequency of the driving voltage is very close to one of the mechanical oscillations of the quartz crystal unit, the amplitude of mechanical vibration will reach a maximum. This method is used in impedance studies of quartz crystals. Such studies are beyond the scope of this thesis but are described in several recent reviews.[8,9] A quartz crystal resonator can also be made to oscillate at one of its resonant frequencies by placing it in the feedback loop of an oscillating circuit

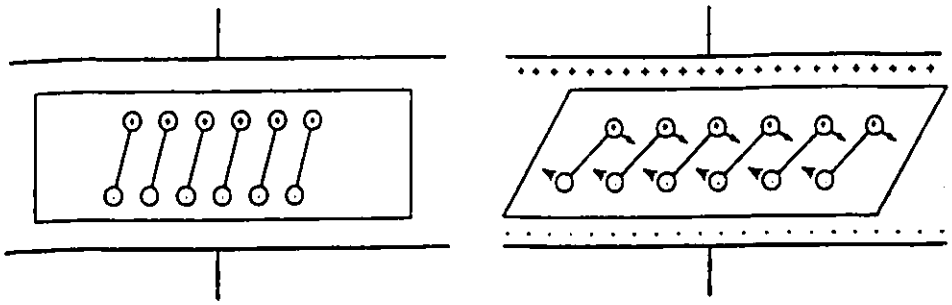

Figure 1. Schematic representation of the converse piezoelectric effect for shear motion. The electric field induces reorientation of the dipoles of the acentric material, resulting in a lattice strain and shear deformation of the material. Direction of shear is dependent upon the applied potential while the extent of shear strain depends on the magnitude of the applied potential (reference 8).

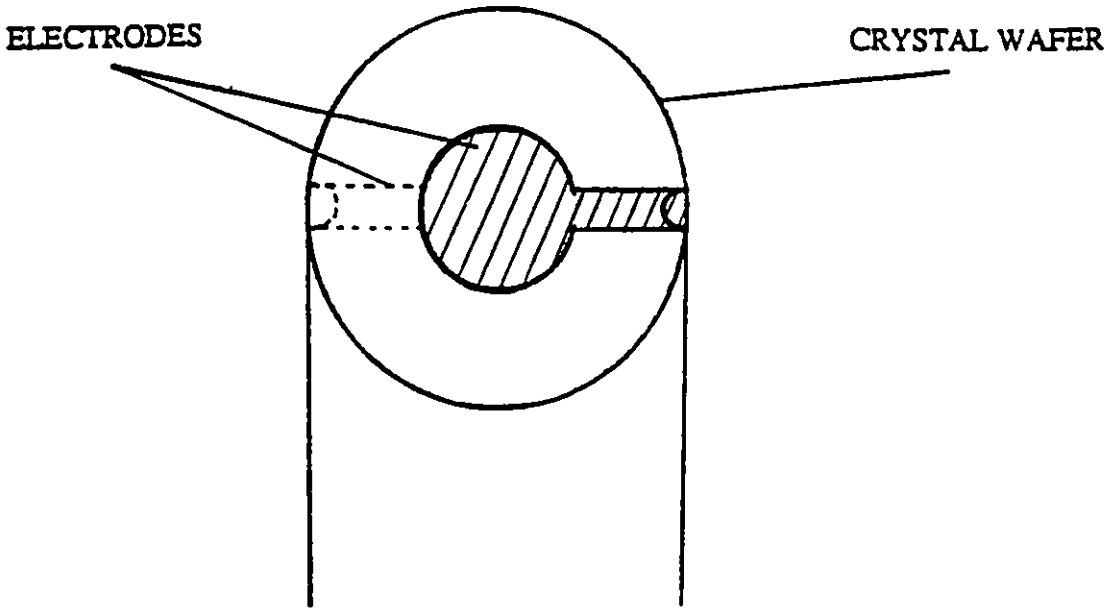

Figure 2. A typical QCM with vacuum deposited electrodes.

containing an amplifier so that it becomes the frequency determining element of the circuit. This method was used in the work reported here.

As with all mechanical structures, a piezoelectric quartz crystal resonator can have many modes of resonance or standing wave patterns at resonant frequencies. The mode of vibration which is most sensitive to the addition or removal of mass for a quartz crystal resonator is the high frequency thickness-shear mode. Thickness shear vibration in the fundamental mode is illustrated in Figure 3. To make a quartz crystal plate oscillate in the thickness-shear mode, the plate must be cut to a specific orientation with respect to the crystal axes. A slight change in the orientation of a quartz crystal plate with respect to the crystallographic axes generally does not alter the mode of resonance. However, the effects of temperature and stress on the resonant frequencies vary with the angle of rotation. Two angles are shown to be insensitive to temperature change in a region around room temperature: $+35^0 15'$ (AT-cut) and $-49^0 00'$ (BT-cut). This is a highly desirable feature for any application that requires the resonator to operate at, or near, room temperature. Figure 4 shows the AT- and BT- cuts which belong to the rotated Y-cut family. The work in this thesis has employed AT-cut crystals oscillating in the thickness shear mode.

iii) The Operating Principle of a QCM in Gas Phase

The operating principle of a QCM for gas phase detection can be described by the

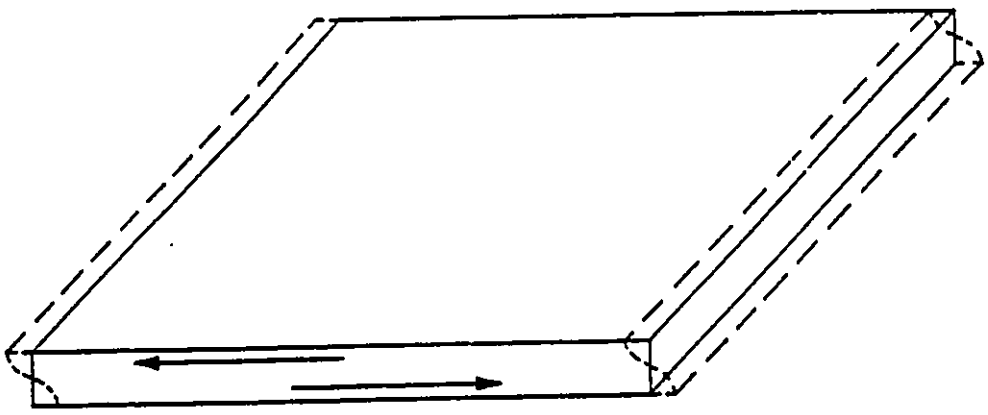

Figure 3. The fundamental thickness-shear mode of vibration (from reference 1).

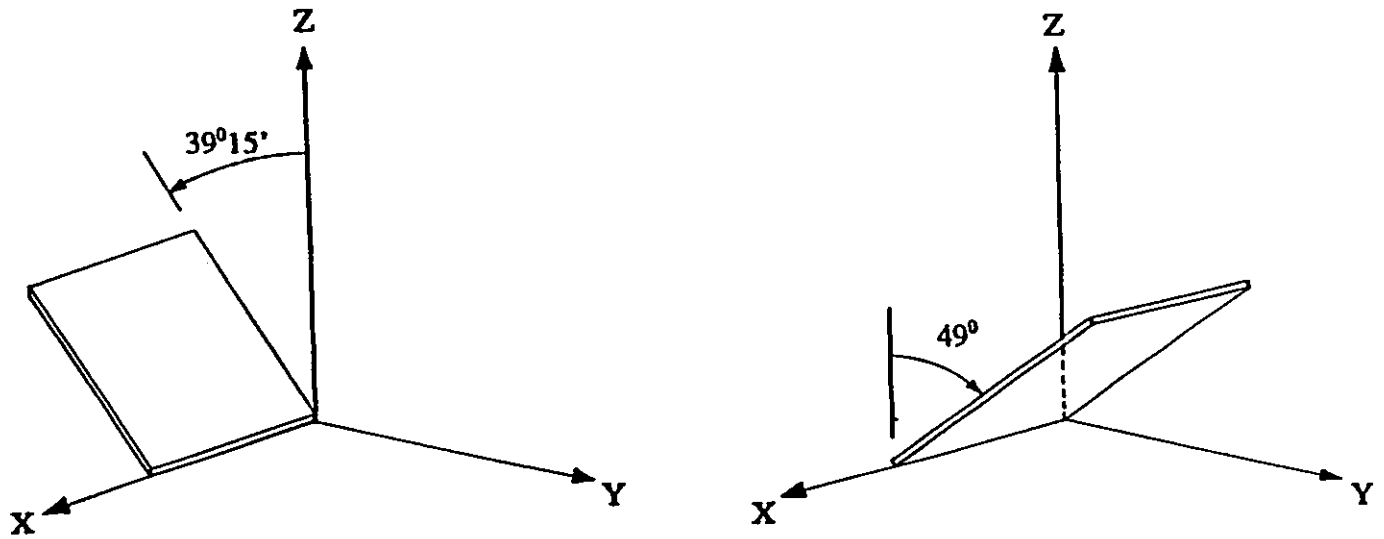

Figure 4. AT- and BT-cut quartz crystal plates (reference 1).

idealized physical model derived by Sauerbrey[7] shown in Figure 5. In order to make a quartz crystal wafer oscillate in the fundamental thickness shear mode, the following equation must be satisfied:

$$t_q = \lambda_q/2 \tag{1.1}$$

where t_q is the thickness of the plate and λ_q is the wavelength of shear-mode elastic wave in the thickness direction. Since the resonant frequency f_q and the shear wave velocity v_q have the following relation:

$$\lambda_q \cdot f_q = v_q \tag{1.2}$$

(1.1) can be written as

$$2f_q \cdot t_q = v_q \tag{1.3}$$

From (1.2) and (1.3),

$$df_q/f_q = - dt_q/t_q \tag{1.4}$$

Because $M_q = t_q \cdot \rho_q$, where M_q is the quartz crystal mass per unit area, ρ_q is the density

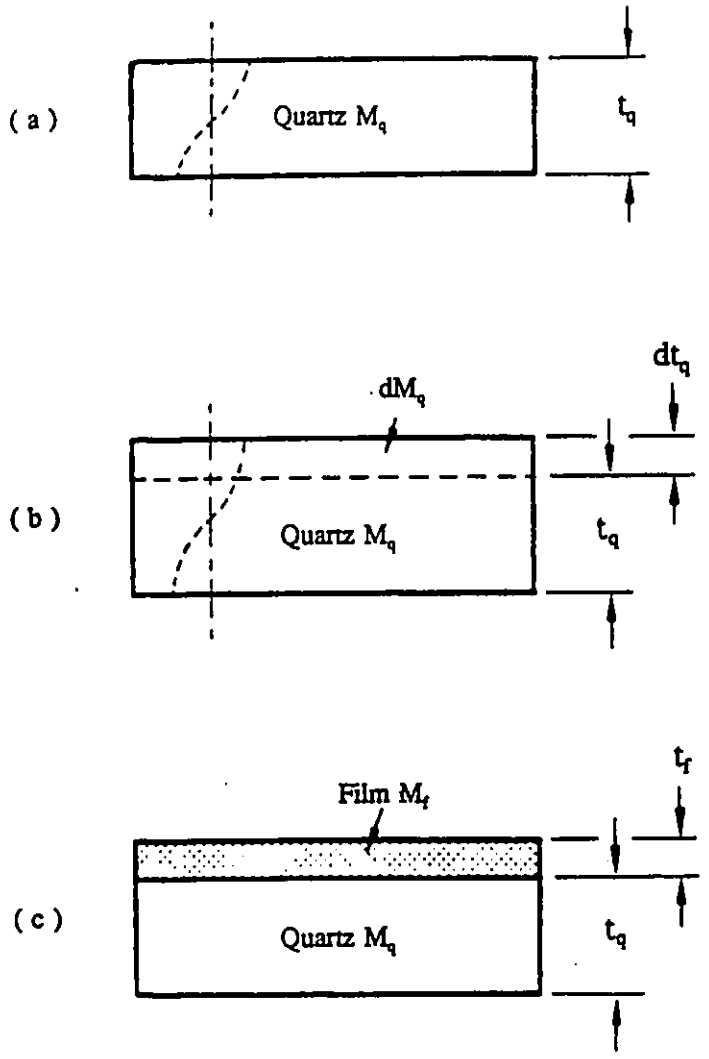

Figure 5. A simplified model of a quartz crystal microbalance. (a) At resonance, the wavelength is equal to twice the quartz plate thickness. (b) An increase in the quartz plate thickness results in a decrease in the resonant frequency (an increase in the wavelength). (c) The mass of a deposited film is treated as an equivalent amount of the quartz mass (reference 1).

of the quartz crystal, equation (1.4) can be expressed as:

$$df_q/f_q = - dM_q/M_q \qquad (1.5)$$

Sauerbrey[7] made the assumption that for small mass changes, the addition of foreign mass can be treated as an equivalent mass change of the quartz crystal itself. Equation (1.5) thus becomes

$$df_q/f_q = - dM/M_q \qquad (1.6)$$

where dM is an infinitesimal amount of foreign mass uniformly distributed over the crystal surface.

Sauerbrey calculated that the change in resonant frequency of the oscillator (Δf) is related to the change in mass (Δm) per unit area (A) of the film for rigid elastic films on the quartz crystal surface:

$$\Delta f = -2 \cdot \Delta m (f_0)^2 / [nA(\mu_q \rho_q)^{1/2}] \qquad (1.7)$$

where f_0 is the fundamental frequency of the crystal, n is the order of the harmonic (overtone number), μ_q is the shear modulus of quartz ($2.947 \times 10^{11} g \cdot cm^{-1} \cdot s^{-2}$), and ρ_q is the density of quartz ($2.648\ g \cdot cm^{-3}$). The negative sign means the mass increases when

the frequency decreases. Equation (1.7) is called *the Sauerbrey Equation.* From this equation, if A = 1 cm^2,

$$\Delta f = -2.26 \times 10^{-6} f_0^2 \cdot \Delta m \qquad (1.8)$$

From equation (1.8), if the fundamental frequency of quartz crystal wafer is 10 MHz, the mass sensitivity is 0.226 $Hz \cdot cm^2 \cdot ng^{-1}$, i.e. 4.42 $ng \cdot Hz^{-1} \cdot cm^{-2}$.

The Sauerbrey equation is appropriate for many situations; however, there are limitations on its use. It is valid only for adlayers of a uniform thickness and for small mass changes (less than a few percent of the mass of the crystal). For thicker, less rigid solids, however, a more complex theory is required[10].

1.1.2. Operation of the QCM in Solution

The QCM which is routinely used in the gas phase may also be used in a liquid environment. There are two simple treatments of the effect of solution on the QCM when one face of the crystal is exposed to the solution.

i) Treatment of S. Bruckenstein and M. Shay

S. Bruckenstein and M. Shay[4] used a treatment analogous to a.c. polarography to

estimate the thickness L of a liquid layer above the crystal that will oscillate with the crystal:

$$L = (\nu/f_L)^{1/2} \tag{1.9}$$

where ν ($cm^2 \cdot s^{-1}$) is the kinematic viscosity of the liquid and f_L (Hz) is the frequency of oscillation of the crystal in the liquid.

The effective additional liquid mass per unit area, Δm, attached to each face of the crystal in contact with the liquid is:

$$\Delta m = \rho_L(\nu/f_L)^{1/2} \tag{1.10}$$

i.e.

$$\Delta m = (\eta_L\rho_L/f_L)^{1/2} \tag{1.11}$$

where ρ_L ($g \cdot cm^{-3}$) is the density of the liquid, η_L is the conventional viscosity of the liquid ($\eta = \nu\rho$). Provided $f_L \doteq f_0$, substitution of equation (1.11) into Equation (1.8) yields:

$$\Delta f = - 2.26 \times 10^{-6} f_0^{3/2}(\eta_L\rho_L)^{1/2} \tag{1.12}$$

for one face of the crystal contacting the solution.

This treatment predicts a frequency decrease of 7 kHz (relative to the value for a crystal exposed to the air) for a 10 MHz AT-cut quartz crystal with one crystal face in contact with solution. This decease arises because of viscosity and density effects. A frequency decrease of this size is typically what was observed for the crystals used in this work.

ii) Treatment of K. Kanazawa and J. Gordon II

Kanazawa and Gordon II[11, 12] used a simple physical model to indicate how the viscosity and density of the contacting liquid affect the oscillation of crystal. This model treats the quartz as a lossless elastic solid, and the liquid as a purely viscous fluid. They examined coupling of elastic waves in the crystal to viscous shear waves in the liquid. This treatment indicates that crystal oscillation gives rise to a highly damped sinusoidal shear wave travelling perpendicularly away from the crystal surface (Figure 6). The treatment suggested that the shear wave in solution would be damped in a distance of ca. 250 nm in water and that the shift in the resonant frequency f_0 caused by immersing one face of the crystal is given by:

$$\Delta f = -f_0^{3/2}[\eta_L \rho_L/(\pi \mu_q \rho_q)]^{1/2} \qquad (1.13)$$

where f_0 is the oscillation frequency of the free (dry) crystal, η_L is the solution viscosity

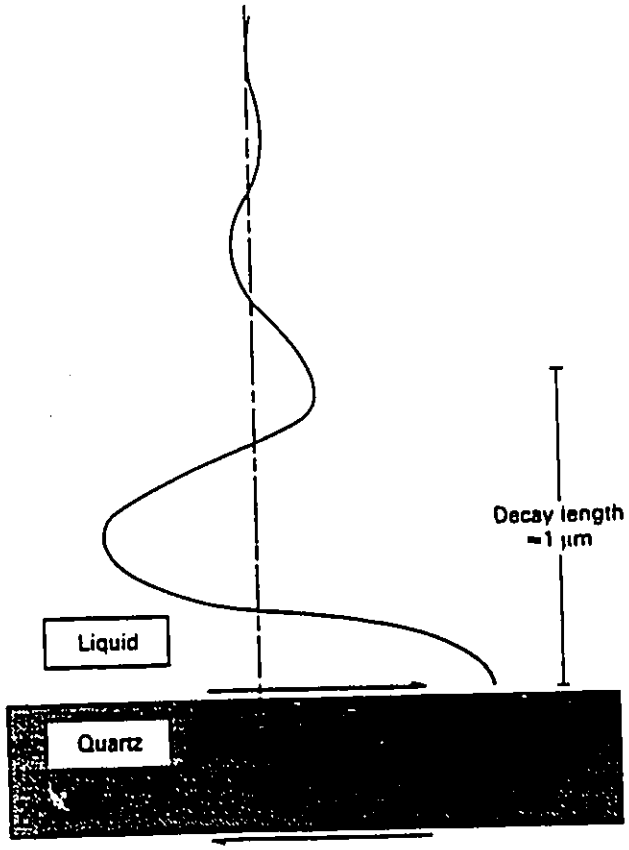

Figure 6. Propagation of the transverse shear wave from the QCM sensor into a liquid (reference 13).

and ρ_L is the density of solution, μ_q and ρ_q are the shear modulus and the density of quartz respectively. By substituting numerical values of μ_q and ρ_q, equation (1.13) can be changed to:

$$\Delta f = -6.39 \times 10^{-7} f_0^{3/2} (\eta_L \rho_L)^{1/2} \qquad (1.14)$$

Equation (1.14) predicts a frequency decrease of 0.7 kHz for a 5 MHz and 2 kHz for a 10 MHz AT-cut quartz crystal respectively with one face in contact with an electrolyte because of viscosity and density effects. In agreement with the model of Bruckenstein and Shay, this model predicts that only a thin layer of liquid will undergo displacement at the surface of the bulk wave device and the device response will be a function of the mass of this layer.

Both treatments indicate that changes in the viscosity and density of the solution will cause a frequency shift, although different values are predicted. The reasons for this discrepancy have not yet been determined. However, the experimental results observed during the course of this work agree with those predicted by Bruckenstein and Shay. Furthermore, if the electrolyte composition and temperature are not changed during the course of the experiment, then there should simply be a constant frequency offset (relative to the case in air) resulting from the presence of solution. Mass changes resulting from addition of rigid deposits to the electrode surface can thus be measured, and treated according to the Sauerbrey equation.

iii) Height of the Solution Contacting the Crystal

As described above the damped shear wave in solution will decay completely in less than 1 μm[11]. Consequently, the amount of liquid contacting the crystal should not influence the frequency of the QCM provided it exceeds this height. This theoretical prediction was tested by Bruckenstein and Shay[4] who measured the frequency of the quartz crystal microbalance after each addition of successive amounts of water to the electrochemical cell to increase the total liquid height up to 11.2 cm. They found that the height of a column of solution above the quartz crystal had a negligible effect on the frequency of a crystal.

Equation (1.8) has been shown to be valid for layers of uniform thickness both in the gas phase and when operating the QCM in solution for a variety of applications. The deposition of a non-rigid (inelastic) film on the QCM can lead to deviations from equation (1.8). However for very thin layers, these deviations are expected to be small. At the solid/solution interface the mass sensitivity is given by equation (1.8). However, moving away from the interface, the sensitivity drops and goes to zero outside of the solution shear wave envelope. Thus if an inelastic layer is confined to a region very close to the solid/solution interface, the sensitivity will be given by equation (1.8). The mass sensitivity has been previously verified by measuring the deposition of various metals from solution in which the current efficiency for deposition is 100%[3,4].

1.1.3. Frequency Changes Not Derived from Mass Changes at the Quartz Crystal Microbalance (QCM)

We have to assume a rigid layer of uniform thickness on the QCM in order to use the Sauerbrey equation. However, in a real situation, some other factors can lead to nonideal behaviour of QCM that causes frequency changes not derived from mass changes. These factors include viscoelastic effects, high mass loading, surface roughness, surface stress, interfacial slippage and nonuniform mass distribution. However, most of these factors have not yet been investigated extensively in the literature, although it has been shown that viscoelastic effects can occur at electrodes coated with adsorbed enzymes or thick polymer films[8]. The possibility of unusual frequency responses arising means that microbalance data should be compared with data from another technique when this is possible.

1.1.4. Electrochemical Quartz Crystal Microbalance (EQCM)

When one of the electrodes deposited on the quartz wafer contacts an electrolyte and also serves as the working electrode of an electrochemical cell (Figure 7), a simultaneous measurement of current-potential and frequency-potential in cyclic voltammetric experiments is possible through the use of an appropriate electric circuit[4]. This arrangement is referred to as the EQCM.

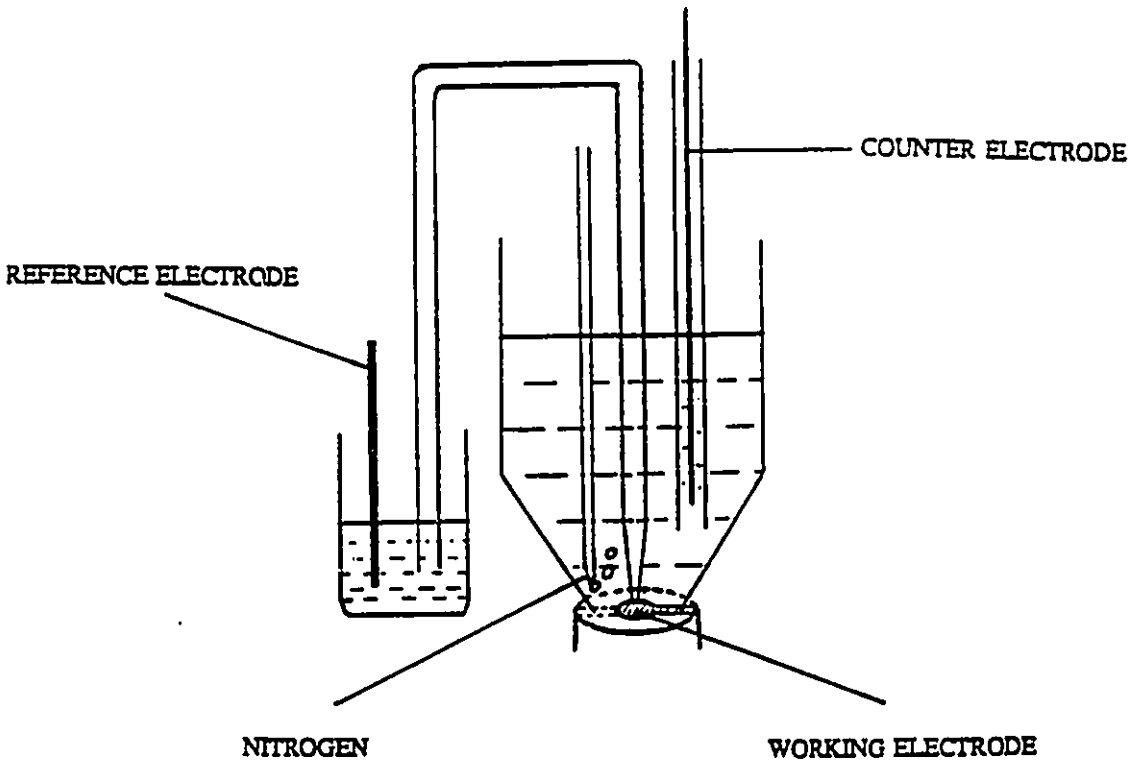

Figure 7. A diagram of EQCM electrochemical cell.

The high sensitivity and characteristic application in solution of the QCM make it ideally suited to study electrochemical processes involving the adsorption of non-electroactive species on the electrode. The EQCM has been used to study monolayer and multilayer processes on electrodes which include the electrosorption of oxides and halides[5,6], underpotential deposition of metals[3,4,14-16] and deposition of polymers[17, 18], dissolution of metals and particularly corrosion[19-22], adsorption of immunoglobulin G[23] and bipyridyl[24], and ion transport into/out of electroactive films[25]. Several papers describing both theoretical aspects of the EQCM and reviewing experimental work are now available.[8,9,26-28]

In this thesis the EQCM has been used to study the adsorption of 4,4'-bipyridyl on gold electrodes.

1.2. Electrochemical Methods for the Study of Adsorption - Differential Capacitance

1.2.1. The Structure of the Electrode-Solution Interface[29-31]

A common electrochemical method for the study of adsorption is differential capacitance, and in this thesis this technique was used to complement information obtained from EQCM experiments. This section describes the structure of the electrode solution interface and explains how capacitance methods can be useful in the study of adsorption.

1.2.2. Introduction

The application of a potential to an electrode in an electrolyte solution causes the surface to take up a characteristic charge and this has electrostatic consequences, oppositely charged ions (and also solvent molecules which in aqueous solution are dipoles) in solution being attracted to the surface; an "electrical double layer" is formed. A representation of the electrode/solution interface is shown in Figure 8.

The value of the surface charge depends on the material of the electrode, the nature of the electrolyte and the potential. Taking the example of the electrode in Figure 8, if the potential is made more negative, electrons will flow into the surface in order to make the surface charge more negative. Conversely, if the potential is shifted towards positive values, electrons will move out of the surface and its charge will become less negative and, eventually, positive. For each electrode/electrolyte combination, there must be one potential where the surface has neither positive nor negative charge and this is known as the potential of zero charge, E_{pzc}. The charge on the electrode surface is always balanced by attracting ions of opposite charge from the bulk solution to the immediate vicinity of the surface. Thus when the potential of an electrode in an aqueous electrolyte is negative with respect to E_{pzc}, its surface will be negatively charged and both cations and dipoles will be attracted to the surface. Conversely, positive to the E_{pzc}, the electrode surface will be positively charged and it is anions and solvent (water) dipoles which are attracted. In practice, anions can be specifically adsorbed at a negatively charged electrode even though

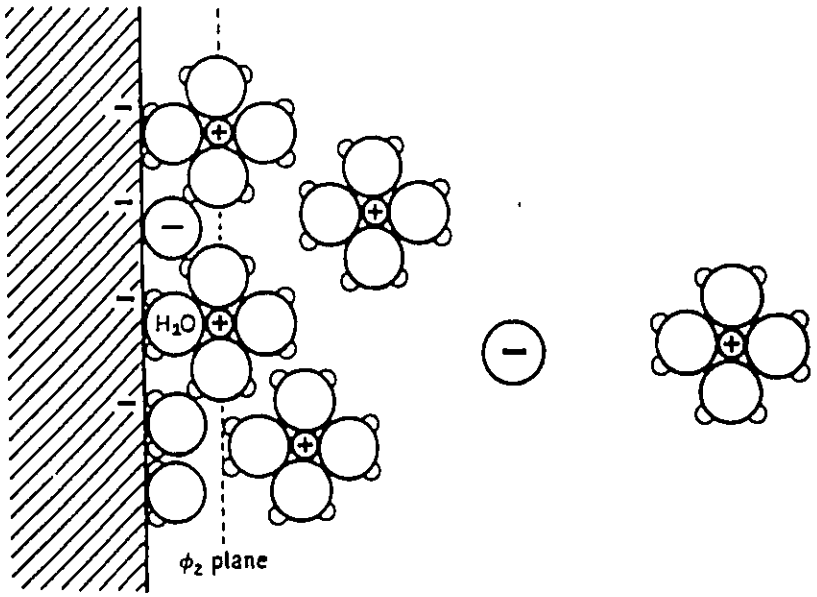

Figure 8. Model of the interfacial region at the electrode surface for potentials negative to the potential of zero charge (reference 31).

the total charge of the double layer is opposite to that of the electrode surface. This is shown in Figure 8. Different anions adsorb to different extent. Anions such as F^- and ClO_4^- do not adsorb strongly whereas the other halides Cl^-, Br^- and ions such as HSO_4^- and $H_2PO_4^-$ are strongly adsorbed.

Next to the local layer of ions and solvent at the electrode surface will be a more diffuse layer of ions of opposite charge. This local layer of ions produces a double-layer which rapidly trails off in the bulk of the solution due to thermal disordering (Brownian motion). The double-layer constitutes a capacitor, capable of storing charge, whose magnitude is of the order of 10 to 100 $\mu F/cm^2$ of electrode surface. Although there is usually a reasonably broad potential region where the double-layer capacitance is approximately constant, it does change with potential and will also be affected by the presence of substances adsorbed at the electrode surface. For example, the displacement of specifically adsorbed ions by neutral organic species will lead to a reduction in the capacitance at the electrode/solution interface. Therefore, measurement of capacitance has been a traditional method used in the study of adsorption of organic molecules on the surface of the electrode.

In the absence of specific adsorption the capacitance of the interface is given by:

$$\frac{1}{C}=\frac{1}{C_i}+\frac{1}{C_d}$$

where C_i is the inner layer capacity and C_d is the diffuse double layer capacity. The contribution of C_d is most visible in dilute solutions where it leads to a sharp minimum

at the potential of zero charge (E_{pzc}). Thus capacitance methods can be used to estimate the E_{pzc} for electrolytes such as NaF or $KClO_4$ where specific adsorption is small.

1.2.3. Adsorption of Organic Molecules

Organic molecules are usually most strongly adsorbed at potentials around the potential of zero charge (E_{pzc}). This is at least partly because adsorption will involve the removal of adsorbed solvent. At potentials away from the E_{pzc} the dipolar solvent is preferentially adsorbed. Similar arguments apply to the competition between adsorbed ions and neutral organic molecules. Because of this competition, capacitance peaks are associated with the adsorption/desorption of organic molecules. For example, Figure 9 shows data for the interface between mercury and aqueous n-pentanol solution. It can be seen that the adsorption or desorption of n-pentanol leads to a big change in the capacitance. The peaks correspond to adsorption/desorption processes and show that n-pentanol is adsorbed between -1.0 V and -0.2 V (very large peaks are associated with desorption if the potential is taken outside this range).

1.2.4. Differential Capacitance

It is clear from the previous discussion that at each electrode/solution interface there

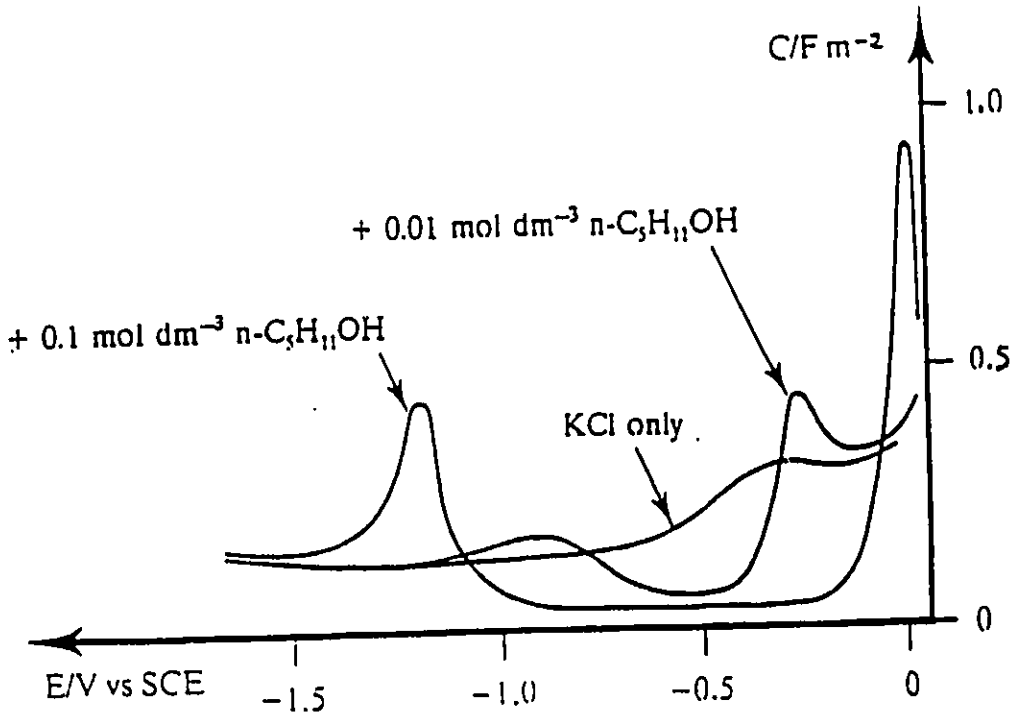

Figure 9. Capacitance-potential curves for n-pentanol at a Hg drop electrode in 0.1 M KCl solution (reference 31).

is a substantial capacitance (C). However, the variation of charge with potential is not often linear and so a differential capacity is defined:

$$C=(\frac{\partial\sigma}{\partial E})_{T,P}$$

where σ is the charge density on the electrode. In the absence of a Faradaic current (a current which is due to the oxidation or reduction of some species), the electrochemical system that consists of a solution resistance and a double-layer capacitance can be represented by a simple resistance-capacitance equivalent circuit in series:

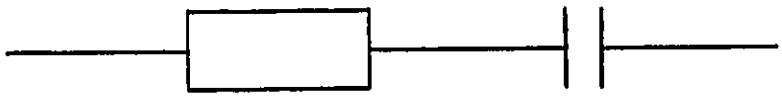

R **C**

where **R** is the resistance of the electrolyte and C means the capacitance of the metal-solution interface. This equivalent circuit model is then used to calculate C as a function of potential as described later.

In the work in this thesis, differential capacitance results have been used to provide information on the adsorption of ions such as ClO_4^-, HPO_4^{2-} and $H_2PO_4^-$ as well as on the

adsorption of 4,4'-bipyridyl. Such data is then compared with information from EQCM experiments.

The experimental arrangement for measuring differential capacitance is described in Chapter 2 and the calculation of differential capacitance is described in the Appendix.

Chapter 2. EXPERIMENTAL

2.1. Electrochemical Quartz Crystal Microbalance and Cell

2.1.1. Electrochemical Instrumentation and Electrodes

An Oxford Electrodes bipotentiostat (Abingdon, England) was used to control the potential and current, voltage and frequency (after conversion to voltage) were output onto an X-Y-Y' recorder (Philips PM8272 or Kipp and Zonen BD 91, Holland). The reference electrode was a saturated calomel electrode (S.C.E.) and the counter electrode was a gold wire. The working electrodes were gold electrodes deposited onto AT-cut, 10 MHz quartz crystals.

2.1.2. Electrochemical Quartz Crystal Microbalance and the Experimental Set Up

The electrochemical cell of the quartz crystal microbalance, and the arrangement of EQCM are shown in Figure 7 and Figure 10. The quartz crystal, mounted on the electrochemical cell using silicone sealant, was connected to a home-made oscillating circuit which is driven by a DC voltage supply (5.0 V). The frequency difference between the working crystal and a reference crystal in the oscillating circuit is monitored with a

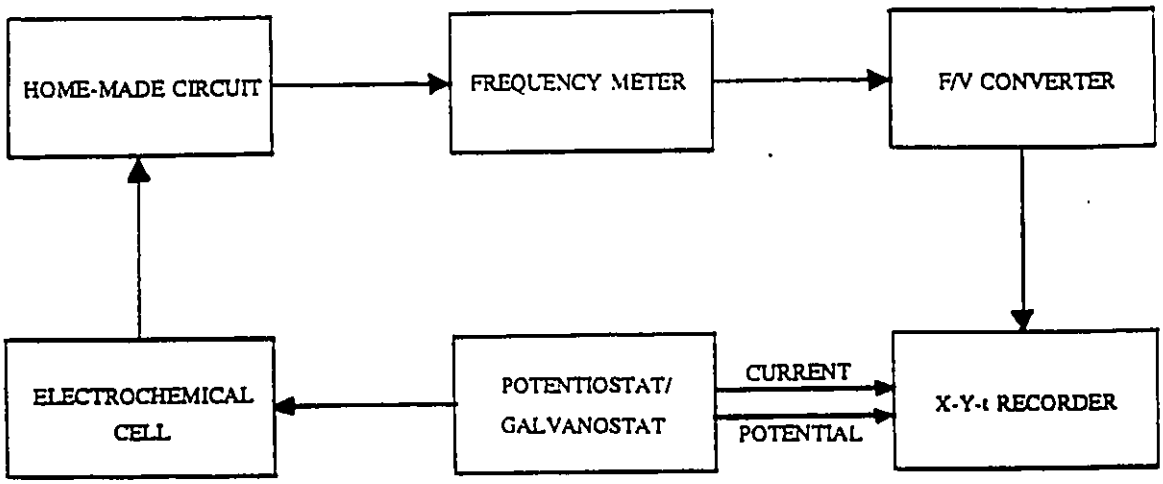

Figure 10. The experimental set up of EQCM.

frequency counter and displayed on a X-Y-Y' recorder after conversion to a voltage by a home-built frequency to voltage converter[4]. A frequency generator was used to perform a frequency to voltage calibration (i.e. to determine how much frequency change corresponds a voltage change of 1 mV). In addition, different pairs of crystals were used as the working and reference crystals and the frequency differences and output voltages recorded. From this frequency and voltage information, the frequency sensitivity was found to be 61.5 mV/kHz or 16.2 Hz/mV.

2.1.3. Calibration of the EQCM

The microbalance (EQCM) was calibrated using galvanostatic deposition of silver on gold in 1 x 10^{-3} M $AgNO_3$, 0.2 M H_2SO_4 (aqueous)[3]. The galvanostatic deposition was carried out at reduction current i_R = 5 μA. Frequency was recorded versus time and the deposited mass was calculated by Faraday's Law.

For the reduction

$$Ag^+ + e = Ag$$

the reduction charge Q may be calculated as the product of the plating time t and reduction current i_R:

$$Q = i_R \cdot t \qquad (2.1)$$

According to Faraday's Law, the mass change during the reduction is

$$m = 107.9Q/96486 \quad (g) \qquad (2.2)$$

where 107.9 is the atomic mass of silver and 96486 (C/mol) is Faraday's constant. The reduction current and the frequency were recorded simultaneously. The relationship between mass and frequency change is shown in Figure 11. The slope, i.e. the mass sensitivity of the EQCM is 1.1 ng/Hz, i.e. 4.4 $ng \cdot Hz^{-1} \cdot cm^{-2}$ (The geometric surface area of the gold electrode is 0.25 cm^2). This value compares well with the theoretical value of 4.42 $ng \cdot Hz^{-1} \cdot cm^{-2}$ calculated from equation (1.8). From the calibration of the frequency to voltage converter, the frequency sensitivity is known to be 16.2 Hz/mV, so the mass sensitivity of the EQCM is 17.8 ng/mV.

2.1.4. Chemicals and Solutions

All solutions were prepared using Millipore Milli-Q water. The chemicals, 4,4'-bipyridyl, NaH_2PO_4, Na_2HPO_4, $KClO_4$ and $HClO_4$ were AnalaR and were obtained from BDH, and were used as received.

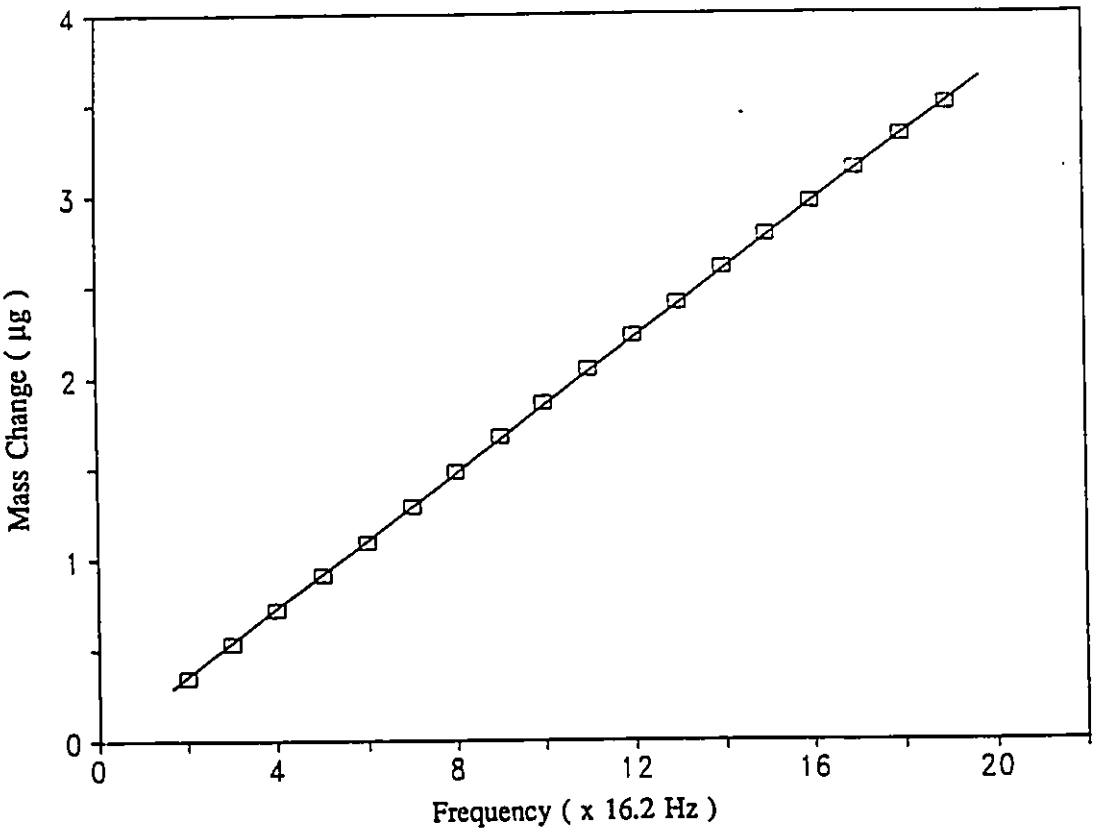

Figure 11. Mass change vs. frequency difference for calibration of EQCM.

2.2. Pretreatment of Gold Electrode and Measurement of Real Electrode Surface Area

Experiments with the EQCM have the advantage of providing an extra piece of information (the variation of the mass of the electrode with potential) alongside the cyclic voltammogram (CV). However, there is also a disadvantage in that the mass response as well as the cyclic voltammogram must be reproducible, and the mass at the end of the experiment should be the same as at the beginning (unless there is a sensible reason why this should not be the case such as dissolution of the electrode or changes in surface roughness[4,32]). We found that the following pretreatment procedure leads to reproducible behaviour from the gold electrodes in phosphate buffers. First, after mounting, the electrodes are cycled in 0.1 M $HClO_4$ between - 0.3 and 1.4 V for the minimum number of scans (about 5) required to produce a reproducible CV. It should be noted that this does not necessarily lead to a reproducible mass response since there is a small amount of dissolution and redeposition of the gold, resulting from repeated oxidation-reduction cycles, in acid media[5,33]. This causes the response of a gold electrode in acid media to change slowly with time.

The real surface area of gold electrode was determined in 0.1 M $HClO_4$ by integration of the charge required for reduction of an oxidised gold surface produced at a potential of 1.2 V (vs. S.C.E.), i.e. one monolayer coverage with O-species, using a charge of 400 $\mu C \cdot cm^{-2}$ [34,35]. An alternative method for surface area measurement is that

of Burshtein et al.[36,37] and involves integration of the charge passed in oxidation of the gold surface in 0.5 M H_2SO_4 electrolyte up to a point in the voltammogram known as the Burshtein minimum. The geometric surface area of the deposited gold electrode is 0.25 cm^2 and typical roughness factors are between 2.5 and 3.5. The electrode is then rinsed and transferred to the solution of interest and cycled through a few more scans until, again, a stable CV is obtained. The mass response resulting from this procedure was found to be reproducible in phosphate buffer.

2.3. Differential Capacitance

Using a two phase lock-in amplifier, the differential capacitance can be measured for each potential applied using equation (A.11). The potential was scanned at a rate of 20 mV/s and a sinusoidal signal of 100 mV amplitude and frequency 16 Hz was superimposed upon it. The values of in-phase (0°) and quadrature (90°) component of a.c. response are the real and imaginary parts respectively.

The schematic diagram of the experimental apparatus is shown in Figure 12. A PAR Lock-in Amplifier (Model 128A) was employed for the differential capacitance measurements. The differential capacitances were calculated from the values of in-phase (0°) and quadrature phase (90°) components of the a.c. current, assuming an equivalent circuit that consists of a solution resistance and a double-layer capacitance in series[38-40] and using equation (A.11) for calculations. Details of the method of calculation are given in the Appendix.

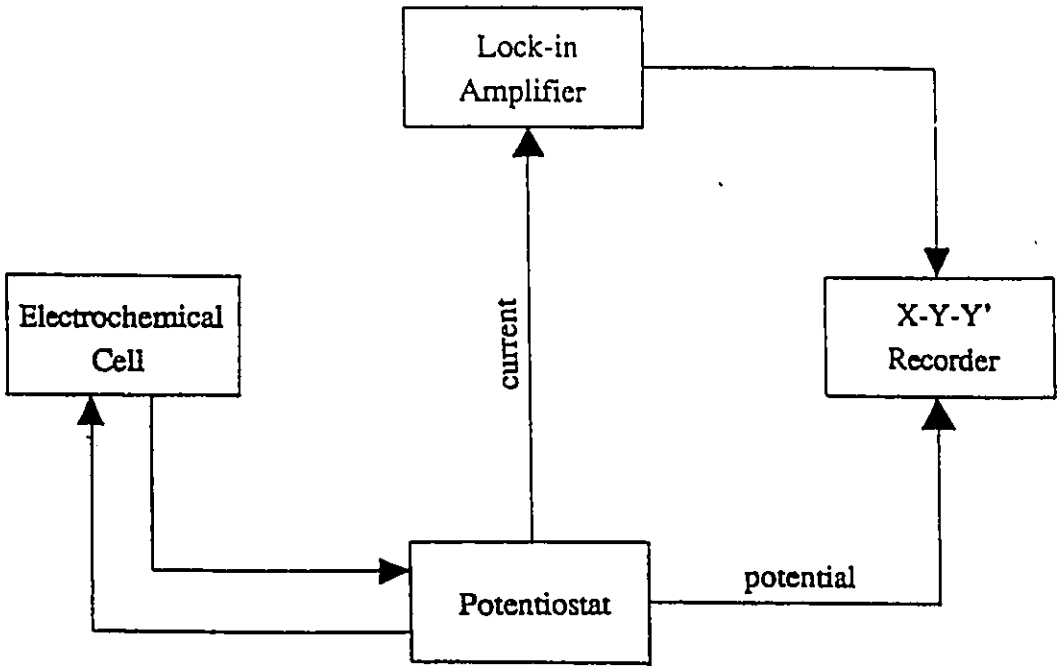

Figure 12. A schematic diagram of the differential capacitance experiment.

2.4. Rotating Ring-Disc Electrode System (RRDE)[29,30,41]

A rotating ring-disc electrode (RRDE) is shown in Figure 13 and consists of three elements: a central disc electrode D (r_1), a ring electrode R (r_2, r_3), and a thin non-conducting gap which separates the disc and ring electrodes. The ring and disc are insulated from one another so that their potentials may be controlled independently. The working surface of both the electrodes and the gap surface lie in one plane and the electrodes are rotated perpendicular to the face of the plane. The rotation of the electrode structure induces a particular flow pattern in the solution which is pulled up at the centre of the rotating structure (i.e. to the disc electrode) and then thrown out radially across the surface (Figure 14). Hence, species formed on the disc are swept out towards the ring; the ring is therefore effectively downstream to the disc and may be used to detect species produced at the disc (Figure 15). Because some of the product formed at the disc will escape into solution, only a fraction of the product will reach the ring to be detected.

The RRDE electrode (shown in Figure 13) was mounted on a bearing block (Oxford Electrodes, England) having a sealed mercury contact. The block was supported on two vertical rods attached to a heavy base to ensure stability. Rotation was controlled by a motor controller (Oxford Electrodes) driving a printed armature d.c. servo motor (Oxford Electrodes). The motor controller display provides an indication of the rotation speed to two decimal places up to a maximum of 50 Hz. The electrochemical cell is shown in Figure 16. A potentiostat (Oxford Electrodes) was employed for the experiment

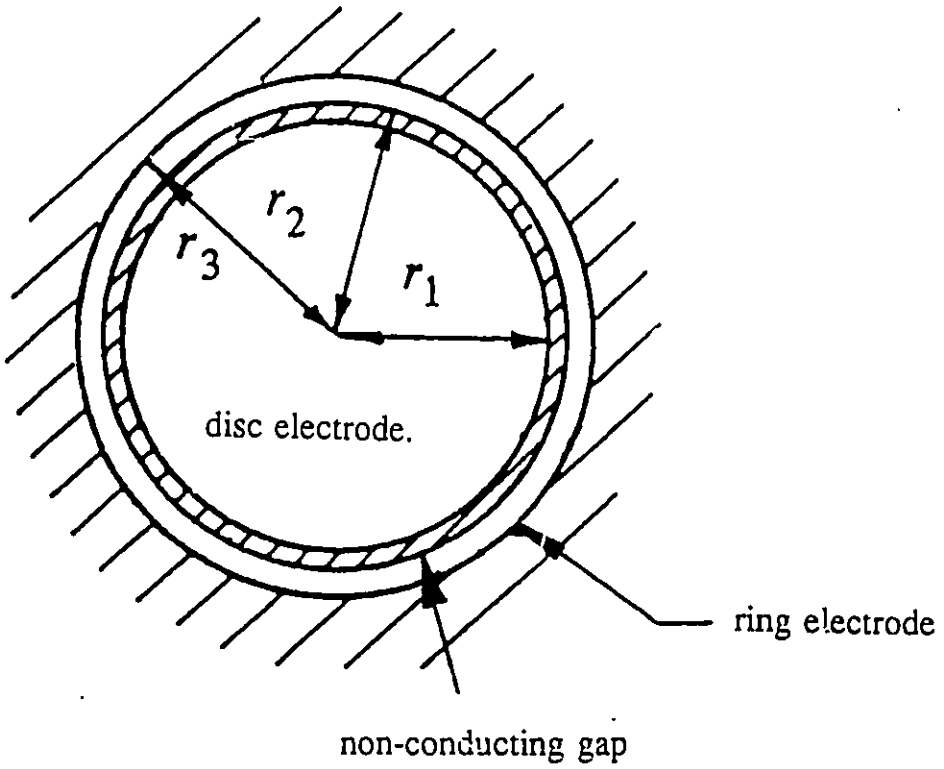

Figure 13. A schematic diagram of the rotating ring-disc electrode.

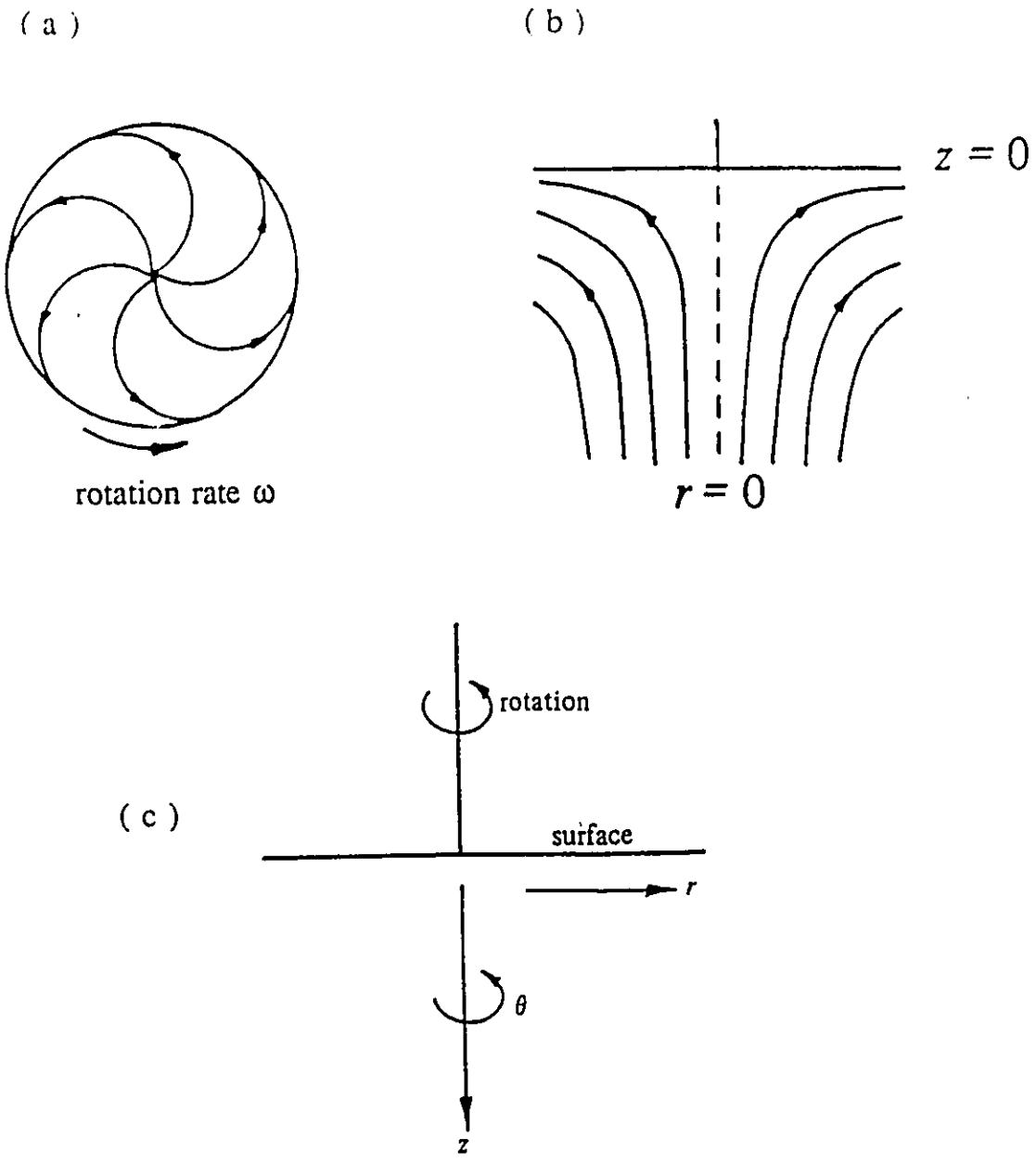

Figure 14. Flow pattern induced by the rotation of the electrode structure.
(a) view from below
(b) view from the side
(c) cylindrical polar coordinates from the rotating disc

(reference 30).

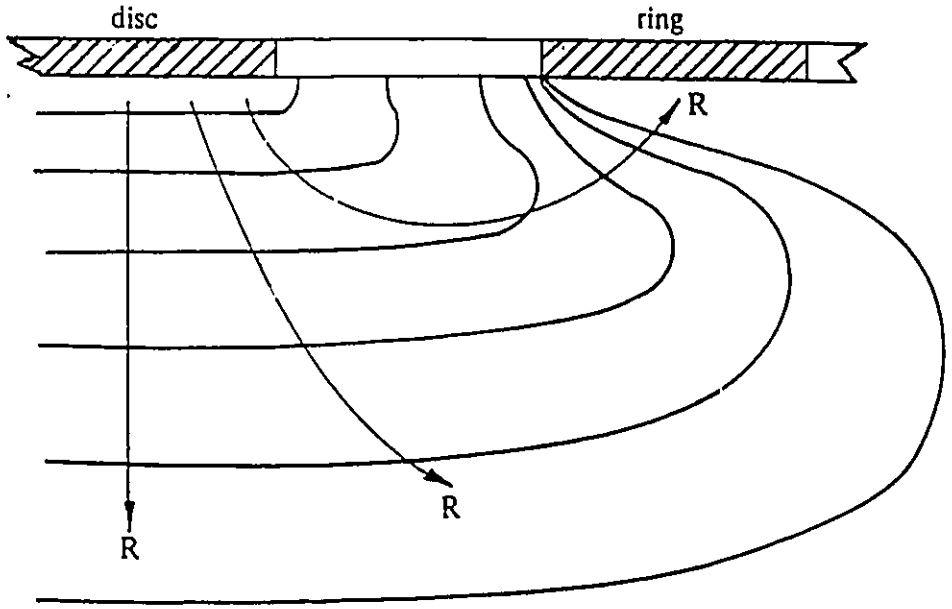

Figure 15. Detection of intermediate product R formed at the disc using ring electrode (reference 30).

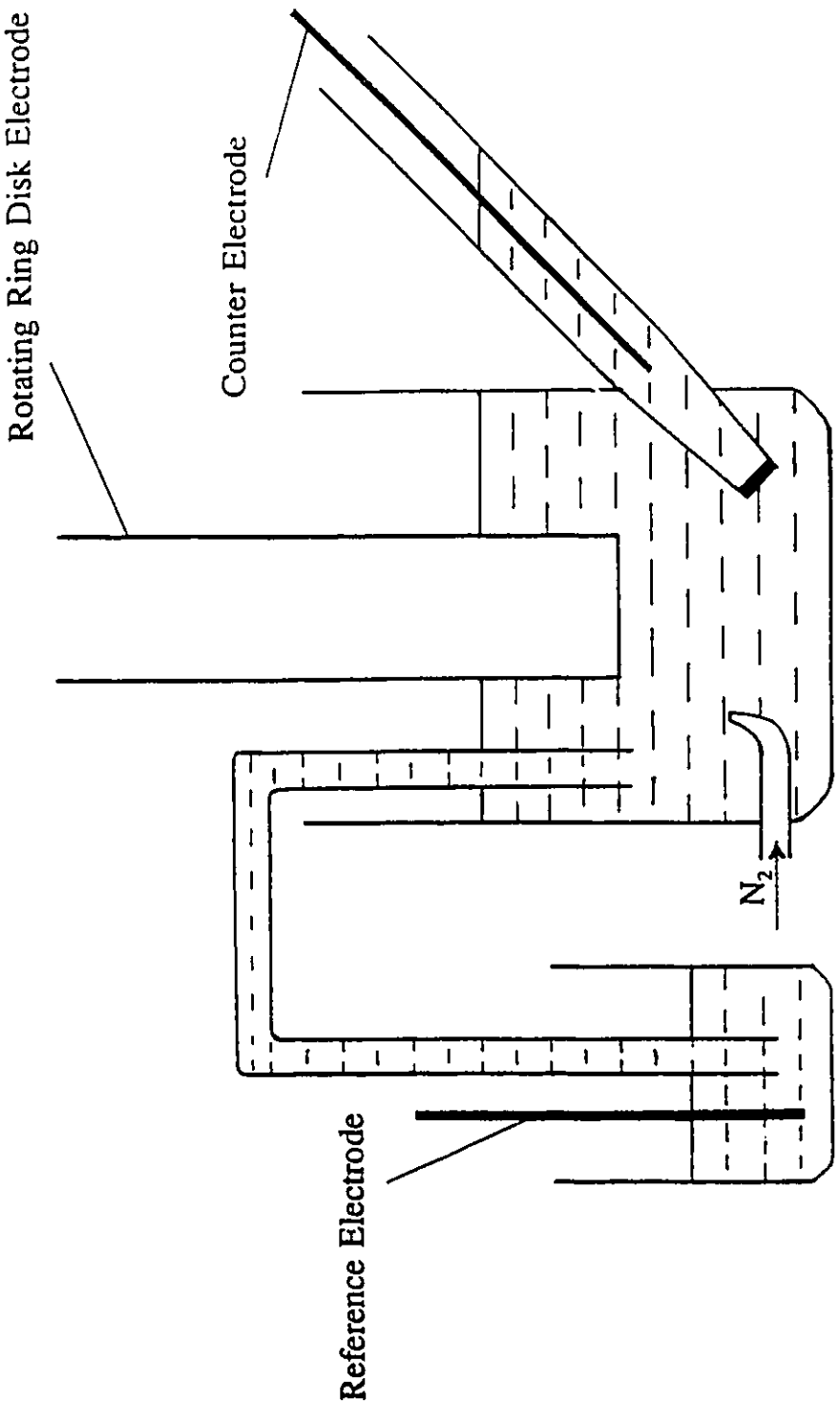

Figure 16. The RRDE electrochemical cell.

and a X-Y-Y' recorder (Kipp & Zonen BD 91, Holland) was used to record the current and potential. A rotating gold disc-gold ring electrode was employed. First, the electrode was polished with Struers alumina paste (fine) and then with 0.06 μ alumina suspension (Struers). Then, the ring-disc electrode was introduced into 0.1 M $HClO_4$, the gold ring and disc were oxidised at +1.5 V for 5 minutes and then reduced at -0.4 V for the same time. Finally, the electrode was cycled repeatedly between -0.3 and +1.4 V at 50 mV/sec until a reproducible cyclic voltammogram was obtained.

Chapter 3. LITERATURE REVIEW

Adsorption of Bipyridyl Molecules at Different Metal Electrodes

3.1. Introduction

Adsorption of organic species at electrodes has applications for a wide variety of electrode processes such as plating, surface finishing and corrosion. For instance, many small organic molecules are used as corrosion inhibitors. Interest in the adsorption of molecules such as bipyridyl arose because of the fact that they act as promoters for redox reactions of small proteins.

It is well known that rapid electron transfer between electrodes and enzymes or proteins is difficult to achieve. This difficulty typically arises because proteins adsorb strongly to electrodes and lose their structure. However, in 1977 Hill and Eddowes[42] found that adsorption of 4,4'-bipyridyl and similar compounds promoted the redox reaction of horse heart cytochrome c, which alone is electrochemically inactive, increasing the electron transfer rate by several orders of magnitude. 4,4'-Bipyridyl and similar compounds which adsorb on the electrode provide a suitable interface for interaction with the protein. Indeed, adsorption of 4,4'-bipyridyl plays a determinant role in promoting the electron transfer reaction between horse heart cytochrome c and an electrode. One view of the mechanism of this promotion is that the adsorption of the 4,4'-bipyridyl at the

electrode surface occurs via one 4-pyridyl-N, while the other 4-pyridyl-N forms hydrogen bonds with lysine ($-NH_3^+$) residues surrounding the heme crevice in cytochrome c. A transient complex is thus formed, allowing electron transfer to take place without the denaturing of the protein which would occur in the absence of the promoter. It has since been found that many other compounds will act in a similar fashion at gold and other noble metals and the general structural requirements for a bifunctional promoter molecule have recently been outlined[43]. Studies have suggested that to act as a promoter, a molecule should have two functional groups. One to help the molecule adsorb, and a second to allow the protein to bind. These should be separated by a rigid link (such as an aromatic ring) to prevent both groups adsorbing at the electrode. However, recent work[44] has shown that molecules that do not fit this model, such as 2,2'-bipyridyl, also can act as promoters, if they are allowed a long enough time to adsorb. This casts doubt on the previous model since 2,2'-bipyridyl would be expected to adsorb through both N atoms and could not offer a functional group to help the protein undergo transient binding.

In this chapter, previous studies of the adsorption of 4,4'-bipyridyl on the metal electrodes including mercury, platinum, silver and gold by different electrochemical methods are summarised.

3.2. Mercury

The mercury electrode was considered ideal for the study of adsorption of organic

substances on electrodes for a long time because of its uniform (and isotropic) surface. In the 1970's, Mambetkaziev et. al.[45, 46] studied the adsorption behaviour of 4,4'-bipyridyl and other bipyridyl isomers at the mercury/water interface by measuring difference-capacitance curves and electrocapillary curves. They found the degrees of coverage (θ) and the Gibbs surface excesses (Γ) by these known techniques. They also concluded that the 4,4'-bipyridyl molecules are adsorbed in a flat position at potentials between -0.1 and -0.8 V vs SCE, and the adsorbate dipoles are parallel to the electrode surface. The 4,4'-bipyridyl molecules reorient from a flat into a vertical position, and form a two-dimensional condensed layer on the surface, when the potential is displaced from this region in the cathodic or anodic direction. The condensed films are formed not only on the negatively charged electrode surface but also at positive electrode charge (at high concentration) for 4,4'-bipyridyl.

The adsorption behaviour of 4,4'-bipyridyl at the solid electrode/water interface has also been investigated by different methods. However most studies of the adsorption of 4,4'-bipyridyl were carried out in the presence of cytochrome c. Often, 4,4'-bipyridyl is adsorbed on an electrode which is then rinsed and transferred to a solution containing either cytochrome c or 4,4'-bipyridyl and cytochrome c. Changes in the cyclic voltammetry of cytochrome c with time are often used to gain information about 4,4'-bipyridyl adsorption. For example if an electrode, with adsorbed bipyridyl present, is transferred to a solution containing only cytochrome c, the current for cytochrome c

oxidation/reduction gradually decreases due to the displacement of 4,4'-bipyridyl by the protein.

A brief review of 4,4'-bipyridyl adsorption at solid electrodes is given below.

3.3. Gold

The orientation of 4,4'-bipyridyl on the electrode surface and the question of whether or not a perpendicular orientation of a bifunctional promoter molecule is required for the promotion of cytochrome c electrochemistry does not yet appear to have been resolved. Uosaki and Hill[38, 39, 47] studied the adsorption of bipyridyl at gold/aqueous solution interface by cyclic voltammetry and differential capacitance and concluded that bipyridyl is adsorbed over a wide potential region from -0.7 to 1.2 V vs. SCE. A small peak in the differential capacitance curve response at about 0.1 V was interpreted as representing the re-orientation of adsorbed bipyridyl between two extreme orientations. Re-orientation of adsorbates such as quinoline at Hg[72] and pyridine at gold[73] has been reported previously and deduced from plots of surface excess (Γ) as a function of potential. Their results for coverage as a function of concentration fitted the Frumkin isotherm. Niwa et al.[48] investigated the adsorption of bipyridyl and cytochrome c on gold by using Infra-red Reflection-Absorption Spectroscopy (IRRAS). The IRRAS study could detect no clear IRRAS spectrum from the gold electrode withdrawn from the 4,4'-bipyridyl solution, only a weak signal around 1600 cm^{-1} was obtained. However, there

was evidence of adsorption of bipyridyl from cyclic voltammetry. A flat orientation of the bipyridyl molecule was suggested from this IRRAS result at the gold electrode surface and 4,4'-bipyridyl molecules were found to be adsorbed weakly at the surface. It was also suggested[49] that bipyridyl molecules in the early stage of adsorption are adsorbed on the layer of water molecules directly adsorbed on the gold electrode. In addition, Surface Enhanced Raman Scattering (SERS) experiments were performed to study the adsorption by Taniguchi and his colleagues[50]. The SERS results indicated that bipyridyl adsorbed onto a gold electrode via the N atom of one pyridine of bipyridyl in the vertical orientation, and a purple-red coloured product was formed due to the reduction of bipyridyl to its anion radical (protonated) formed at potentials more negative than -0.8 V vs. SCE. More recently, Czerwinski et al.[49] studied the adsorption of 4,4'-bipyridyl on gold electrode by electrochemical methods in both neutral and acidic solutions. They concluded that the adsorption is a one-centre reaction involving displacement of water molecules from metal surface. The adsorbed molecules are perpendicularly oriented towards the electrode surface. They also found that the time of exposure of the electrode to promoter was significant for 4,4'-bipyridyl and deduced that the adsorption (carried out in their work at 5°C) involved initial coordination to surface water which is eventually displaced by bipyridyl, leading to a stronger adsorption at longer time (several hours). The adsorption obeyed the Langmuir-type isotherm.

3.4. Platinum

The behaviour of 4,4'-bipyridyl on platinum was investigated by Taniguchi and his colleagues[51] as well as Gui and Kuwana[52].

Taniguchi et. al. obtained a quasi-reversible redox wave for cytochrome c at platinum in the presence of 4,4'-bipyridyl. In order to get reliable results, they pretreated the electrode by sweeping in the potential range between 0.5 (or 0.6) and -0.7 (or -0.9) V vs SCE for more than 20 cycles in the buffer solution containing 4,4'-bipyridyl, to produce what they described as a reduced and activated surface. They noted that a higher concentration of bipyridyl was required to obtain voltammetry of cytochrome c at Pt when compared to gold. The electrode was also found to become deactivated if the potential was taken to values greater than 0.6 V (S.C.E.).

Another group, Y. Gui and T. Kuwana, has studied the adsorption of bipyridyl and other electrochemically inactive, heterocyclic aromatics on a smooth clean platinum electrode by long optical path length thin-layer spectroelectrochemistry. They found that the adsorption of these aromatics is irreversible and potential-independent on a clean platinum surface from an aqueous solution. By comparing calculated and experimental values for the area occupied by adsorbed 4,4'-bipyridyl, they suggested that it was adsorbed in both flat and vertical orientations and that the orientation may be concentration dependent, changing to a completely vertical orientation at higher concentrations.

3.5. Silver

The behaviour of 4,4'-bipyridyl on silver electrode is different from other metal electrodes. Cotton and her colleagues [53, 54] studied the behaviour of 4,4'-bipyridyl on silver electrodes using cyclic voltammetry and surface-enhanced Raman Scattering (SERS). They observed enhancement of the electron-transfer rate between cytochrome c and a silver electrode in the presence of 4,4'-bipyridyl. Their results indicate that 4,4'-bipyridyl interacts strongly with the silver surface and inhibits the adsorption of cytochrome c onto silver. During an oxidation reduction cycle in 0.1 M Na_2SO_4 with 1 x 10^{-2} M 4,4'-bipyridyl, a peak near + 0.3 V (vs. SCE) was observed which was attributed to the formation of Ag(I)-4,4'-bipyridyl complex in the diffusion layer and on the electrode surface. The complex is reduced at potentials near + 0.1 V and - 0.06 V (vs. SCE) (two reduction peaks due to different structures). They also found that multilayers of the complex formed on the electrode surface during the reduction and are desorbed during oxidation of 4,4'-bipyridyl.

3.6. Summary

Despite some disagreement between different workers the following points can be made with regard to the adsorption of 4,4'-bipyridyl.

1. 4,4'-Bipyridyl is adsorbed over a wide potential range, particularly at gold

electrodes.

2. The orientation of adsorbed bipyridyl is not well defined and may depend on concentration and possibly potential.

3. Adsorption seems to be weak since activity for redox reactions of cytochrome c is lost unless 4,4'-bipyridyl is present in solution with the protein. Several workers have suggested that initial coordination may be through surface water[50].

Chapter 4. RESULTS AND DISCUSSION

4.1. Introduction

In this chapter, the results of an EQCM study of the adsorption of 4'4-bipyridyl at gold electrodes are presented. The background electrolyte for this work was 0.1 M $KClO_4$ in 0.02 M phosphate buffer at pH = 7.0. Since the individual components of the buffer solution, particularly the phosphate and perchlorate anions, are capable of adsorption, the microbalance response was first examined in $HClO_4$ and $KClO_4$ to investigate the effect of ClO_4^- and then in $KClO_4$ solutions to which phosphate was added to investigate the effect of phosphate ions, before the adsorption of 4,4'-bipyridyl was studied. Both differential capacitance and microbalance techniques were used.

EQCM studies of the electrosorption of monolayer systems involving small molecules are an extremely challenging application of the technique for several reasons.

i) Mass changes are generally small, although this depends on the MW (molecular weight) of the species involved in the process giving rise to a mass change. For example a monolayer of deposited Pb will be easily detected whereas a monolayer of adsorbed H atoms may not. Further complications arise because in addition to the electrosorption event, several other processes may contribute to the observation of frequency changes.

ii) The structure of the electrode/solution interface described in Chapter 1 (Figure 8) reveals that any adsorption of neutral organic molecules will displace ions or water, so mass changes will be made up of two contributions. The first from species adsorbed, and the second from species displaced. Therefore processes such as adsorption/desorption of solvent or supporting electrolyte ions occurring during the electrosorption will contribute to the observed mass changes.

iii) Finally, other processes such as changes in the position of the slip plane (i.e. the plane which defines the first layer of the adjacent medium which is not rigidly attached to the electrode surface) due to the electrosorption, and changes in the viscosity and/or density of the double layer induced by changes in composition as a function of applied potential may also influence the frequency changes of the EQCM.

However, because the adsorbate layer is so thin compared to the wavelength of the shear wave in the resonator, the added mass from the electroadsorbed layer should exist entirely at the antinode of the shear wave. Therefore, the adsorbate layer should experience no significant shear deformation, and its viscoelastic properties should have no influence on the measurement.

4.2. EQCM and Differential Capacitance Results for Gold Electrodes in the "Double Layer" Region of Potential in Perchlorate Solutions

Experiments were performed in both acidic ($HClO_4$) and neutral ($KClO_4$) solutions

of perchlorate. Experiments in $HClO_4$ solutions were carried out to reproduce literature data before proceeding to $KClO_4$ solutions. The double layer region of potential is the region between hydrogen evolution and the potential at which the oxidation of the electrode surface begins. The only process of interest here is the possible adsorption of ions from the background electrolyte. As the following discussion will show, examination of the literature reveals a general agreement that perchlorate ions have only a weak specific adsorption at gold at potentials positive of the E_{pzc} (potential of zero charge).

Adsorption from $HClO_4$ and $KClO_4$ solutions was studied by Clavilier and Huong[40] using differential capacitance and cyclic voltammetry methods. They found similar differential capacitance-potential (C-E) curves in $HClO_4$ and $KClO_4$ solutions and concluded that $E_{pzc} = -0.040 \pm 0.010$ V vs S.C.E. independent of pH or concentration, so there is little specific adsorption of ClO_4^- in this potential range. However a slight specific adsorption of ClO_4^- was suggested at more positive charge densities at potentials positive of E_{pzc}.

Hinnen et. al.[55] performed differential capacitance experiments in different electrolytes: $KClO_4$, NaF, KCl and Na_2SO_4. From their results, the adsorption strength of anions at gold electrodes in the double layer potential region was suggested to be $ClO_4^- < F^- < SO_4^{2-}$ and Cl^-. Borkowska and Stimming studied adsorption from $HClO_4$ solutions over a range of concentration and concluded that the E_{pzc} didn't change with concentration and that there was a weak adsorption of ClO_4^- at potentials positive of the pzc.

Similar conclusions were reached after work on single crystals. In 1986, Conway

et. al.[56] studied gold single crystal planes by the potentiodynamic sweep method in $HClO_4$ and H_2SO_4 solutions. They found that in the double layer potential region, there was a specific adsorption of the anions accompanied by partial or full charge transfer, and the adsorption of anions was weak in $HClO_4$ and strong in H_2SO_4 solutions.

As the first part of the work in this thesis the behaviour of the evaporated gold electrode of the EQCM was studied in 0.1 M $HClO_4$. Figure 17 shows the experimental result of a differential capacitance experiment on the EQCM gold electrode in 0.1 M $HClO_4$ solution. From the differential capacitance-potential curve, the capacitance is seen to have a small change in the double layer region of potential, and the capacity minimum is a little negative of 0.00 V. This indicates that the E_{pzc} is at a potential which is a little negative of 0.00 V. This value is consistent with that found by Clavilier and Huong[40]. The differential capacitance-potential curve also indicates that there is a slight adsorption of perchlorate anion on the electrode in the double layer region of potential, but from Figure 18 it may be seen that there does not appear to be any significant current that could be assigned to partial discharge of adsorbed ClO_4^-. This may be compared to the results observed in a phosphate containing electrolyte (see Figure 25).

4.3. EQCM Studies of Gold in the Region of Potential Where the Electrode Surface is Oxidised

Oxidation of gold and platinum in general follows a similar mechanism with

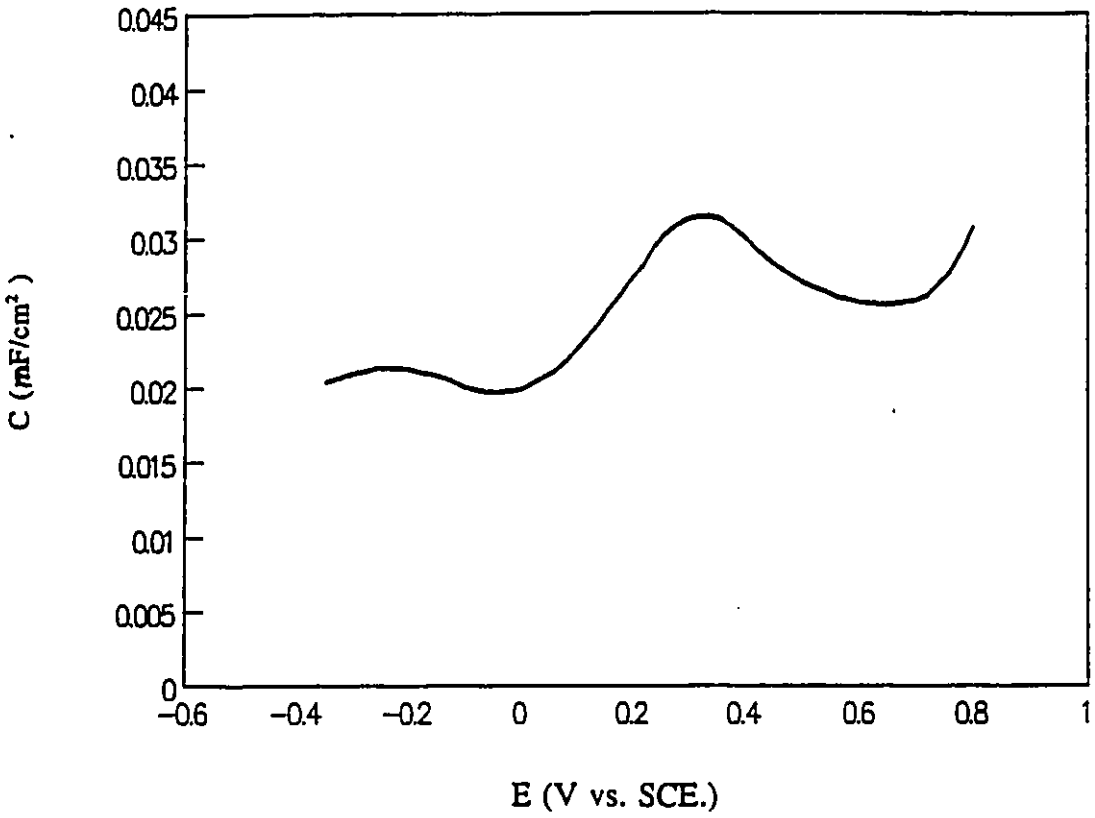

Figure 17. Differential capacitance-potential curve of EQCM gold electrode in $HClO_4$ solution.

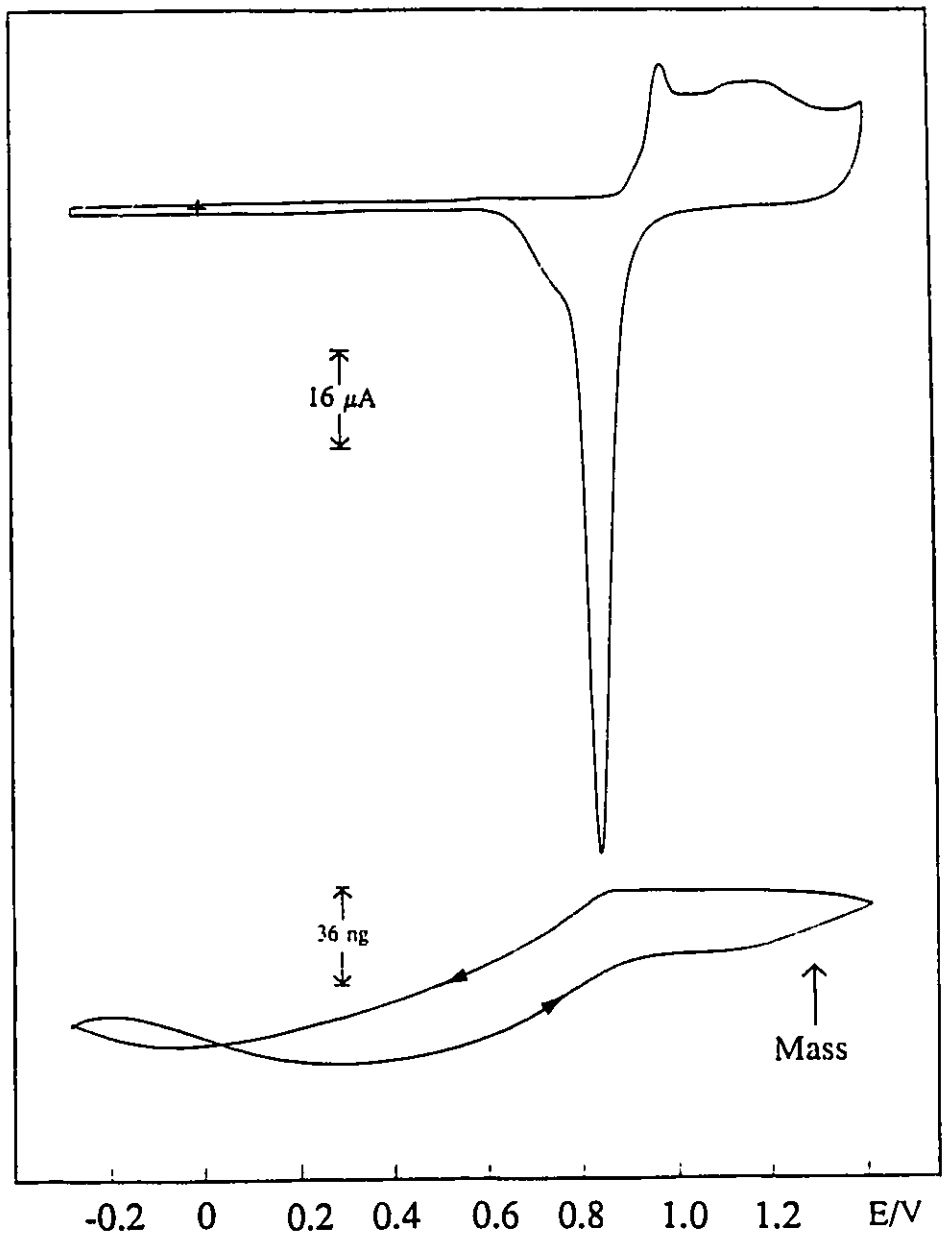

Figure 18. A cyclic voltammogram and mass response for the EQCM gold electrode in 0.1 M $HClO_4$ solution. Scan rate = 20 mV/s.

successive discharge of adsorbed water followed by a place exchange process. The role of adsorbed anions is ignored here.

e.g.

$$M(H_2O)_{ads} \rightarrow M\text{-}OH + H^+ + e^- \quad (4.1)$$

$$M\text{-}OH \rightarrow HO\text{-}M \quad (4.2)$$

$$HO\text{-}M \rightarrow O{=}M + H^+ + e^- \quad (4.3)$$

$$O{=}M + H_2O \rightarrow O{=}M(H_2O)_{ads} \quad (4.4)$$

Processes (4.2) and (4.4) represent place exchange where the O atom or OH inserts itself into the lattice. When the electrode surface is reduced the O or OH re-emerges from the lattice. The oxidation/reduction mechanism of Au in 0.2 M $HClO_4$ was one of the first systems studied using the EQCM. Brnckenstein and Shay[5] compared the mass change observed on oxidation of gold with the change expected from charge, assuming a mechanism such as that shown below:

$$Au(H_2O)_{ads} \rightarrow Au\text{-}OH + H^+ + e^- \quad (4.5)$$

$$Au\text{-}OH \rightarrow Au{=}O + H^+ + e^- \quad (4.6)$$

$$Au{=}O \rightarrow O{=}Au \quad (4.7)$$

$$O{=}Au + H_2O \rightarrow O{=}Au(H_2O)_{ads} \quad (4.8)$$

First, there is a successive oxidation of adsorbed water to generate Au=O (Equations (4.5), (4.6)), followed by place exchange (Equations (4.7), (4.8)) and readsorption of water. According to this mechanism, the net effect of oxidation is simply the insertion of a layer of O into the gold lattice, Au-$(H_2O)_{ads}$ becomes O=Au-$(H_2O)_{ads}$. This mechanism was established by determining the in situ change in weight of the gold electrode together with the cyclic voltammogram using the quartz crystal microbalance method. Bruckenstein and Shay calculated the amount of the oxidation both from the mass response of the EQCM and from the charge and found values of (20.1 ± 0.04) x 10^{-9} g and 18.3 x 10^{-9} g respectively. They also found that in solutions stirred by bubbling nitrogen a small amount of gold was lost into solution on oxide reduction. A comparison of charge and mass showed that about 40% of the total charge was passed before the mass began to increase. This was attributed to the initial step being proton loss(Equation (4.5)) which is too small to detect in the mass signal.

A cyclic voltammogram and mass response for the EQCM gold electrode in 0.1 M $HClO_4$ solution is shown in Figure 18. The mass change calculated from the frequency changes is very close to the mass change predicted from charge measurements. Our results are in agreement with those of Bruckenstein[5]. An experiment was also carried out in 0.001 M $HClO_4$ solution (Figure 19). The recorded frequency curve is quite flat in the double layer region of potential which means the mass change in this region is quite small in 0.001 M $HClO_4$ (note that the scales of Figures 18 and 19 are different). It is indicated from the different results of EQCM in 0.1 M $HClO_4$ and 0.001 M $HClO_4$

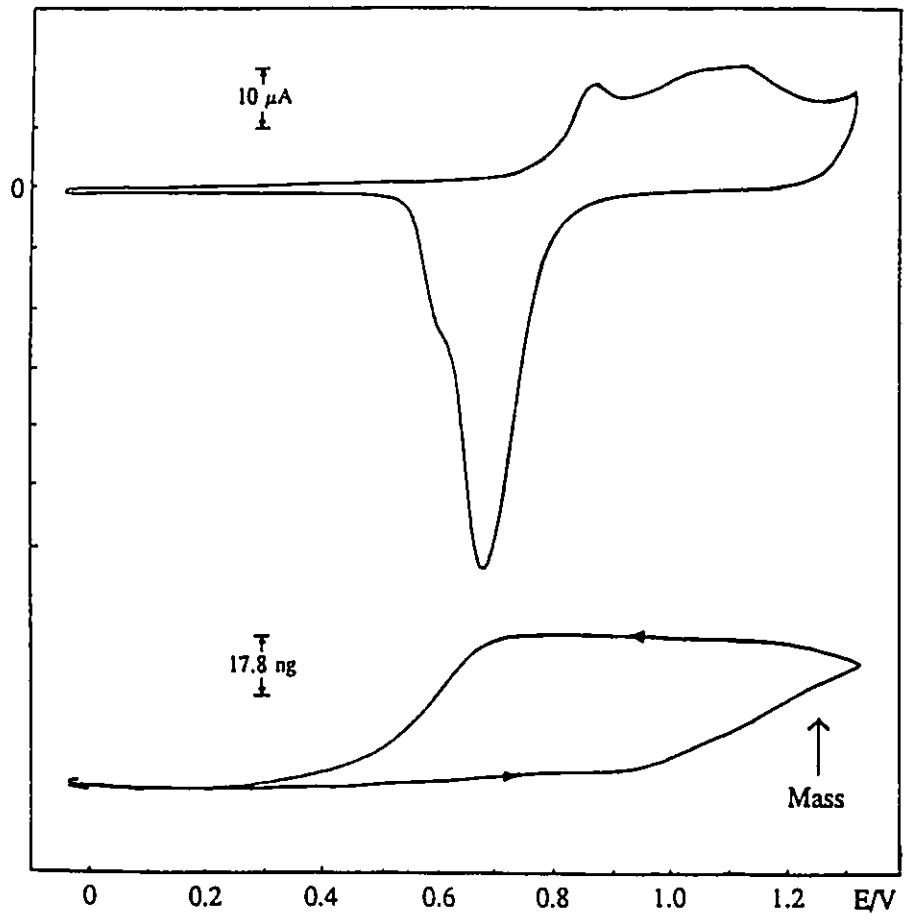

Figure 19. A cyclic voltammogram and mass response for the EQCM gold electrode in 1.0 x 10^{-3} M $HClO_4$ solution. Scan rate = 20 mV/s.

solutions that the supporting electrolyte (anions) has an influence on the frequency changes in the double layer region of potential.

4.4. The Behaviour of the Gold Electrode in Potassium Perchlorate Solution

4.4.1. The "Double Layer" Region of Potential

A cyclic voltammogram and mass response of the EQCM gold electrode in 0.1 M $KClO_4$ between -0.6 and 0.6 V vs. SCE. are shown in Figure 20. The region of potential used here corresponds to the double layer region of potential, and there is no oxidation or reduction of the electrode surface, but at the negative limit of the scan there is a small current increase in the positive direction and a small decrease in the reverse direction. This current is due to the reduction of traces of oxygen in the solution. The mass change accompanying this voltammogram is flat between 0.6 and 0.0 V but increases at potentials below the E_{pzc}. The differential capacitance of gold electrode in 0.1 M $KClO_4$ was also measured. The result is shown in Figure 21, which agrees with the results of Hinnen[55], Clavilier[40] and their colleagues. From the differential capacitance-potential (C-E) curve, it can be seen that the C-E curve is quite close to that in perchloric acid (Figure 17) and the minimum capacity is around 0.00 V which relates to the E_{pzc}. There are two differential capacitance peaks at -0.2 V and 0.3 V which relate to the small current increase from CV curves, and the capacitance values of the peaks are quite small.

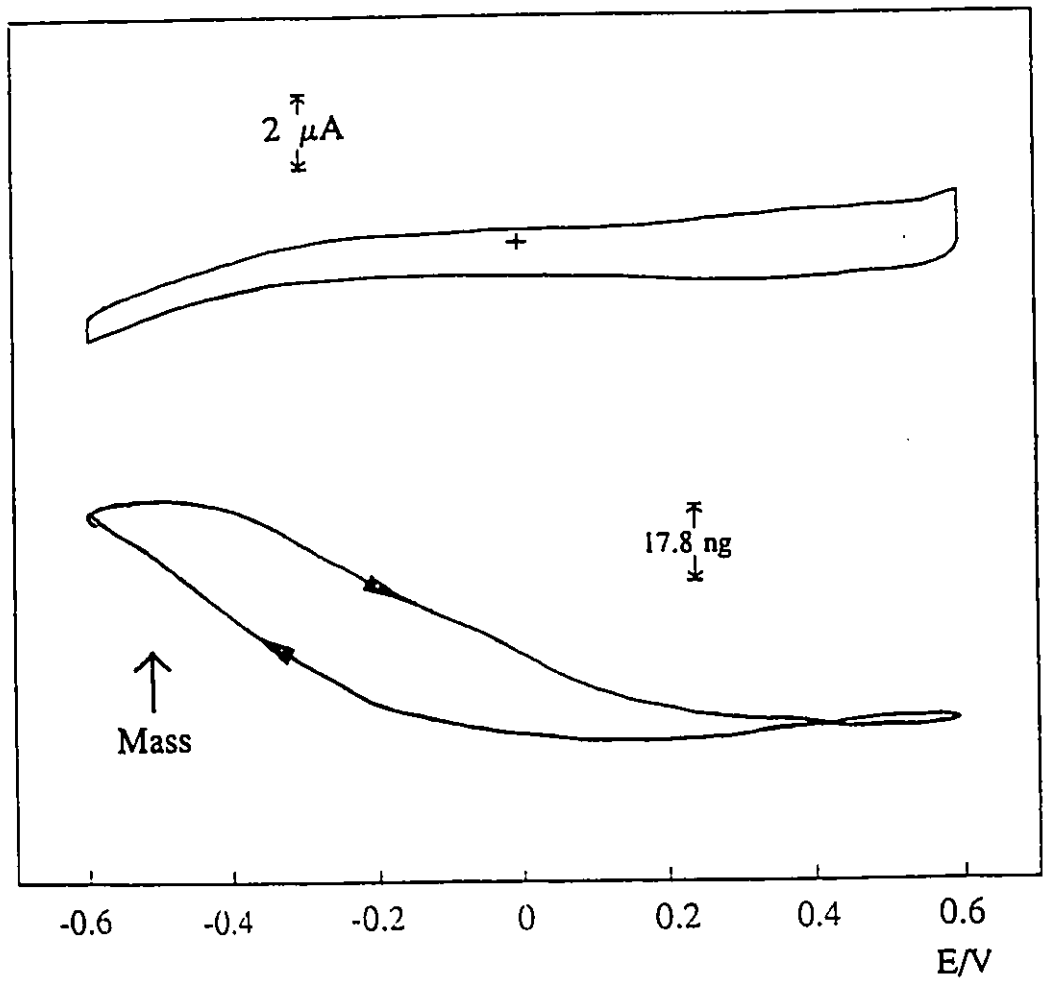

Figure 20. The cyclic voltammogram and mass response of the EQCM gold electrode in 0.1 M $KClO_4$ solution. Scan rate = 20mV/sec.

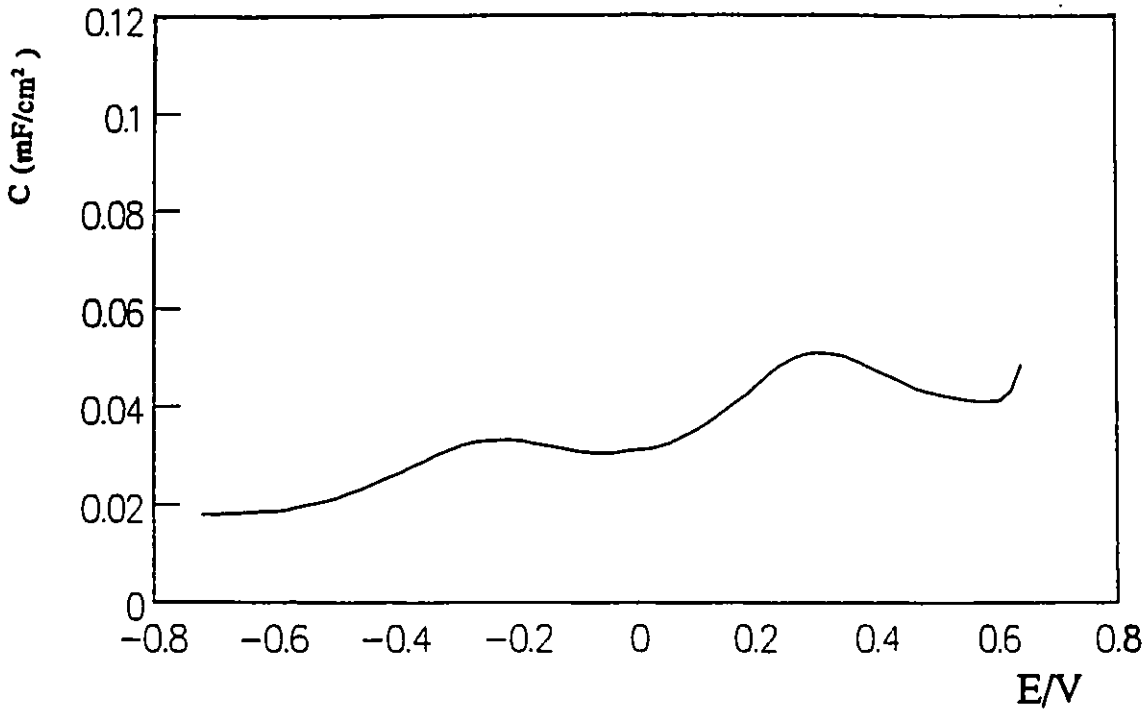

Figure 21. Differential capacitance-potential curve of the EQCM gold electrode in 0.1 M $KClO_4$ solution. Scan rate = 20 mV/s, frequency = 16 Hz.

Therefore, it may be concluded that the deposited gold electrode of the EQCM behaves similarly to a bulk gold electrode and that the perchlorate ions have only a weak adsorption in the double layer region of potential.

4.4.2. Cyclic Voltammetry and Mass Response in the Region of Potential Where the Electrode Surface Is Oxidised

The cyclic voltammograms of an EQCM gold electrode in 0.1 M $KClO_4$ solution at room temperature under stationary and purging nitrogen conditions between -0.6 and 1.2 V (vs. SCE.) are different (Figure 22). The differences are similar to those observed at a platinum electrode[57] (in 1 M Na_2SO_4 solution) under similar conditions. L. Stolberg et. al[58] also observed the same results in 0.1 M $KClO_4$ solution at the Au(111) electrode. These differences arise because of the involvement of protons (see mechanism on p.56) in the oxidation/reduction of the electrode in what are unbuffered neutral solutions.

When the electrolyte is purged with nitrogen, the two peaks in oxidation region are just slightly higher than those seen in stationary solution, however the reduction region is quite different. Under purging nitrogen conditions, the result is similar to that seen in acidic solutions in that there is only one reduction peak which appears at about 0.2 V, while the oxidation region in the stationary solution is not. In the stationary solution, there are two reduction peaks: one is at about 0.22 V (peak B) and another is at about 0.67 V (peak A).

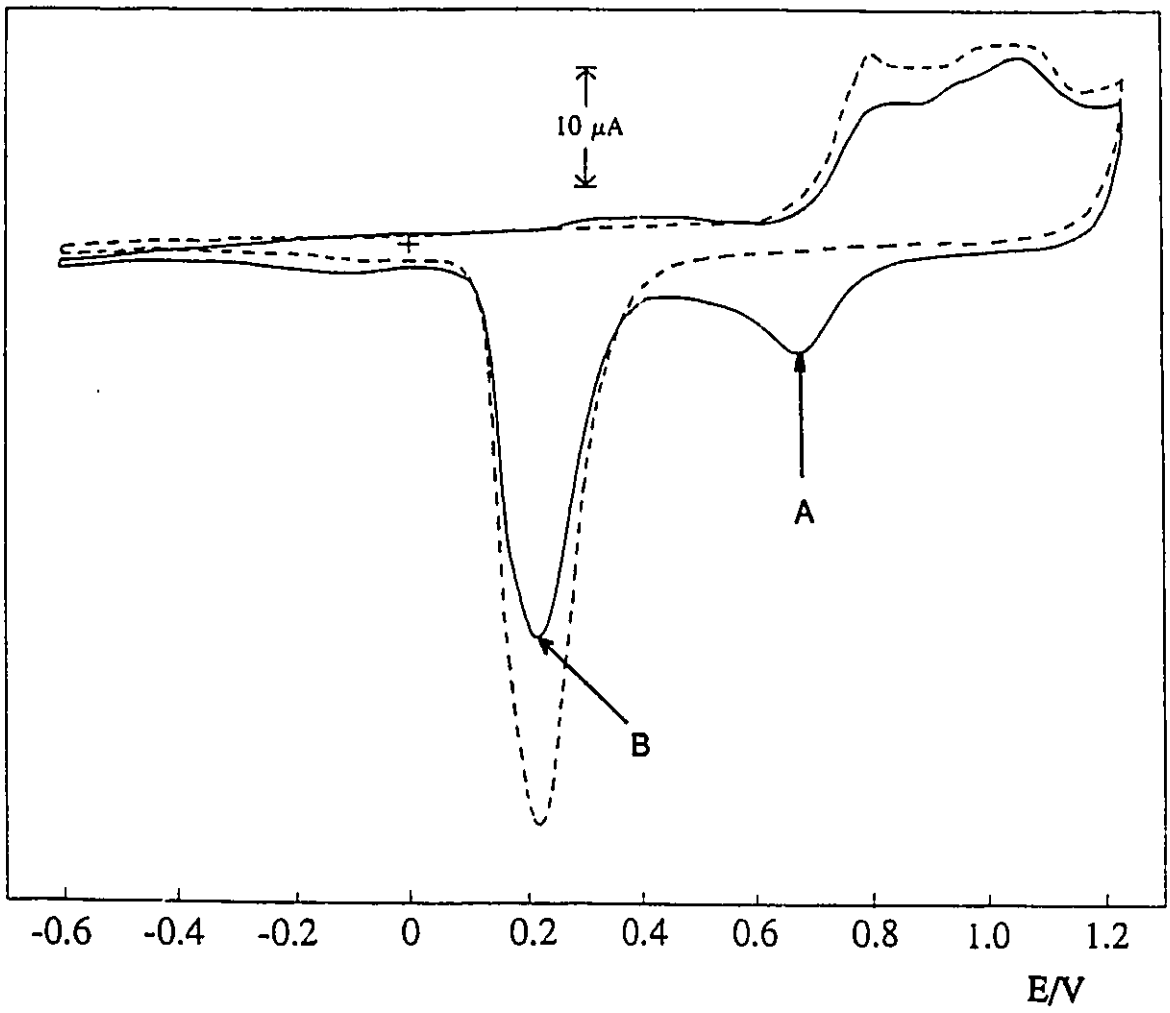

Figure 22. Cyclic voltammograms of an EQCM gold electrode in 0.1 M $KClO_4$ under stationary (solid) and purging nitrogen (dashed) conditions. Scan rate = 20 mV/s.

A possible mechanism for the oxidation of the gold electrode is shown below[5]:

$$Au\text{-}(H_2O)_{ads} \rightarrow Au\text{-}OH + H^+ + e^- \quad (4.9)$$

$$Au\text{-}OH \rightarrow Au{=}O + H^+ + e^- \quad (4.10)$$

Possible processes[58] leading to reduction peaks (A) and (B) in a stationary solution are:

$$Au{=}O + 2H^+ + 2e^- \rightarrow Au + H_2O \quad (4.11)$$

$$Au{=}O + H_2O + 2e^- \rightarrow Au + 2OH^- \quad (4.12)$$

Reaction (4.11) involves protons in solution, whereas reaction (4.12) will result in OH^- diffusing away from the electrode. This would indicate that reaction (4.11) is due to a change of pH in the vicinity of the electrode surface caused by the local excess of protons produced by the oxide formation process. This local excess is removed when protons are transported into the bulk of the solution by purging nitrogen. Figure 23 shows a mass response corresponding to the stationary condition in 0.1 M $KClO_4$, for the whole potential range including oxidation and reduction of the electrode surface.

Four points can be noted from the mass response.

a) There is a mass increase observed as the potential is scanned below 0.0 V. When

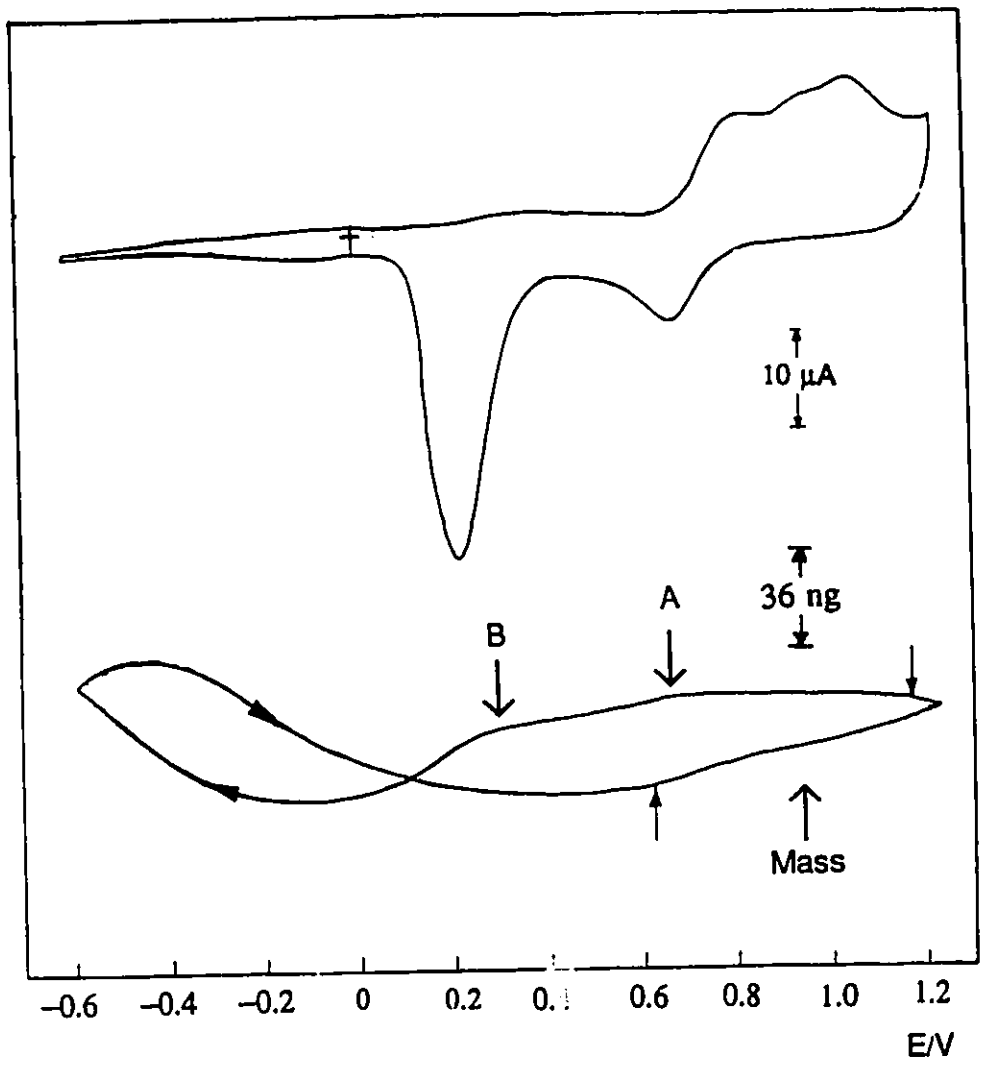

Figure 23. The cyclic voltammogram and mass response of the EQCM gold electrode in 0.1 M $KClO_4$ solution under stationary condition. Scan rate = 20 mV/s.

the potential is reversed at -0.6 V there is then a mass decrease. This change is similar to that shown in Figure 20.

b) Between the potentials of 0.0 and 0.6 V on the positive-going scan there is no mass change. This can be compared with the increase in mass seen in the double layer region of potential in 0.1 M $HClO_4$ (Figure 18).

c) The mass increase upon oxidation of the electrode (indicated as being the arrows on Figure 23) is 32 ng and agrees quite well with the mass change expected from charge calculations (27 ng).

d) Interestingly there are two small steps in the mass response on the reverse cycle (indicated by arrows A and B in the Figure 23) which seem to correspond to the two reduction peaks in the stationary solution.

Figure 24 shows an experiment where the potential was cycled from the negative limit of -0.3 V to successively increasing upper limits in stationary solution. From Figure 24, it may be deduced that the mass change from 0.6 to 1.2 V is caused by the oxidation of the gold electrode. As the potential increases above 0.6 V, the extent of oxidation of the electrode surface increases and the mass also increases. On the reverse cycle, the mass decrease from 1.0 to 0.1 V results from the reduction of the oxidised gold surface.

4.4.3. Summary

1. Differential capacitance results in 0.1 M $HClO_4$ and 0.1 M $KClO_4$ agree well

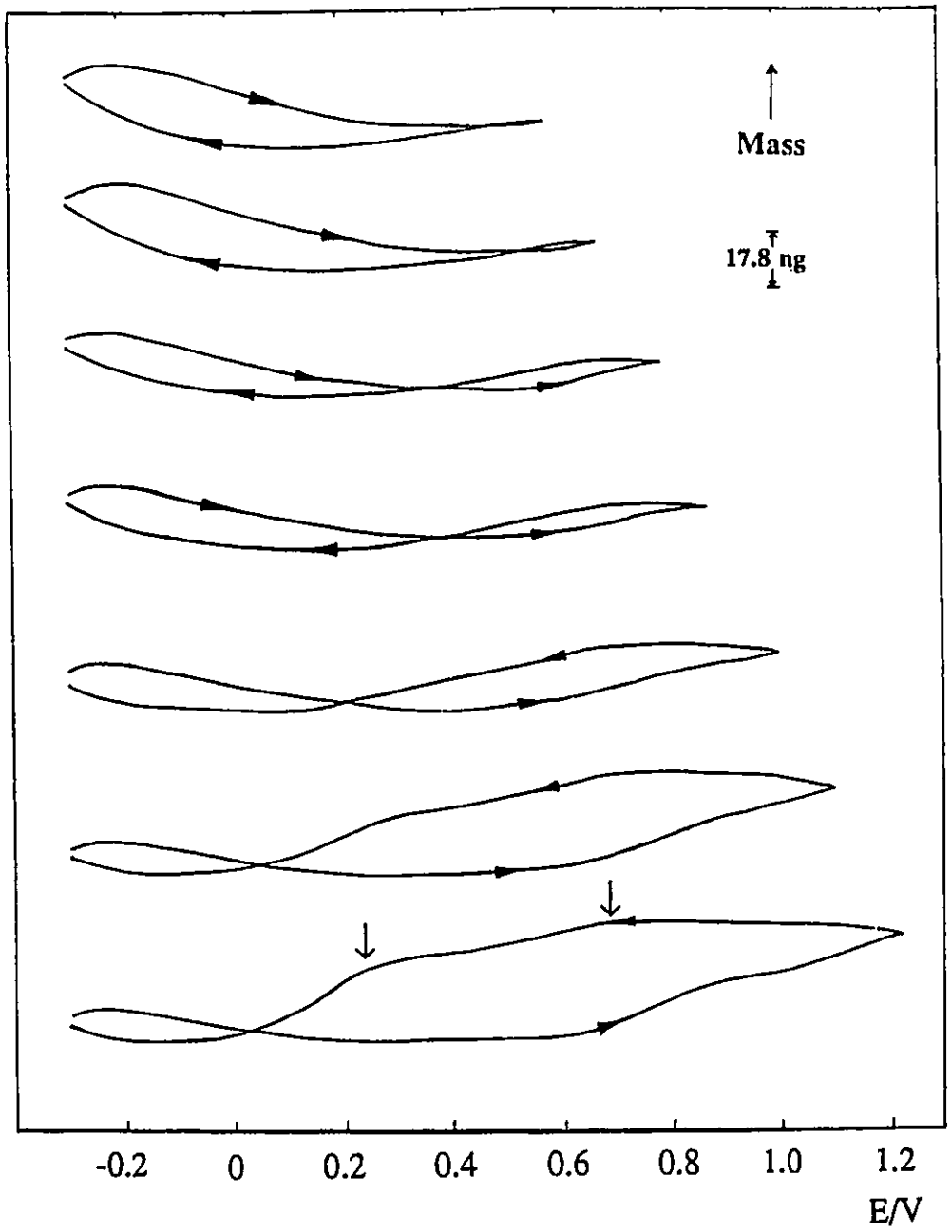

Figure 24. The mass response of the EQCM gold electrode in 0.1 M $KClO_4$ solution. Scan rate = 20 mV/s. The anodic potential limit was taken to successively more positive potential for 7 cycles.

with published literature data, and indicate a weak adsorption of ClO_4^- ions at potentials greater than the E_{pzc}.

2. EQCM results show that at potentials greater than the E_{pzc} in both 0.001 M $HClO_4$ and 0.1 M $KClO_4$ there is no change in mass observed, which is consistent with point 1, until the electrode surface oxidation begins.

3. At potentials greater than the E_{pzc} in 0.1 M $HClO_4$ the mass does increase with potential. While this is consistent with literature results, the reason for the difference in behaviour between 0.1 M $KClO_4$ and 0.1 M $HClO_4$ is not known.

4. At potentials below the E_{pzc} mass increases with decreasing potential for all solutions. Possible causes for this change will be discussed later.

4.5. The Adsorption of Phosphate at the Gold Electrode

The effect of phosphate ions on differential capacitance, voltammetry and mass responses was studied here because it is known to adsorb more strongly than perchlorate on electrodes.

4.5.1. Literature Review - Phosphate Adsorption

The literature regarding phosphate adsorption on gold is not extensive. Most studies have been conducted in acid solutions. In 1972, Takamura and Takamura[59]

presented results of reflectivity measurements of the electrosorption of halides, phosphate, sulphate and nitrate anions on a gold electrode in 0.2 M $HClO_4$ in a short communication. They concluded that the presence of H_3PO_4 in 0.2 M $HClO_4$ enhanced the decrease of reflectivity in the double layer region of potential due to the adsorption of phosphate on the gold electrode. They also found that the order of the extent of adsorption of anions in acidic media on a gold electrode is: $I^- > Br^- > Cl^-$ > phosphate > sulphate and nitrate but did not give any details. Bockris[60] et. al. also presented an FTIR study of adsorption from aqueous solutions of phosphoric acid onto Pt and Au. They found that the adsorption increased up to 1.2 V vs. NHE (ca. 0.8 vs. SCE) and then decreased upon further increase of potential. The decrease in coverage of the H_3PO_4 species is due to the displacement by the oxide layer which is formed significantly above about 1.1 V vs. NHE (ca. 0.7 vs. SCE). K. Takamura, Mori and Watanabe[61] also observed the adsorption of phosphate at gold electrode at -0.2 V vs. SCE when they studied the adsorption of adenine derivatives on gold by specular reflectivity measurements.

Another group, Florit, Martins and Arvia[62], studied the behaviour of some systems including KH_2PO_4/H_3PO_4, H_2SO_4/Na_2SO_4, $HClO_4/NaClO_4$, H_2SO_4/HCl on gold in acidic media. They observed that the acid electrolyte compositions had inhibiting effects on the O-electroadsorption on gold and explained the inhibiting effect which happened in the double layer region of potential in terms of a potential-assisted interaction of the different anions in solution with the gold surface, producing a blockage of sites for the early stage of the O-electroadsorption from water. They suggested that the following process takes

place at the double layer region of potential:

$$(+)Au(H_2O)_y + A^-(H_2O)_x \rightleftharpoons (+)Au(A^-)(H_2O)_{x'} + y'H_2O \qquad (4.13)$$

where the parentheses correspond to adsorbed species and $x + y = x' + y'$. Once the adsorption equilibrium is established, the discharge of water yielding adsorbed oxygen and protons might occur either on $Au(H_2O)$ or $Au(A^-)H_2O$ sites. They concluded that the inhibition of the O-electroadsorption was attributed to the specific adsorption of anions through the competitive process indicated by reaction (4.13) and the extent of the influence of $H_2PO_4^-$ and HPO_4^- is much greater than ClO_4^-.

It may be concluded from the discussion above that phosphate ions are adsorbed on the gold electrode and that this adsorption is stronger than that of ClO_4^-.

4.5.2. Phosphate Adsorption at Gold Electrode in the Double Layer Region of Potential

Figure 25 shows a cyclic voltammogram and mass response for the double layer region of potential in 0.1 M $KClO_4$/0.02 M phosphate (pH = 7.0) system. The current-voltage curve reveals two pairs of small current peaks (ca. -150 mV and 170 mV) (Figure 25) when recorded on a sensitive scale. These two pairs of peaks were observed on a variety of gold electrodes including the EQCM gold electrode and gold wire and gold disc

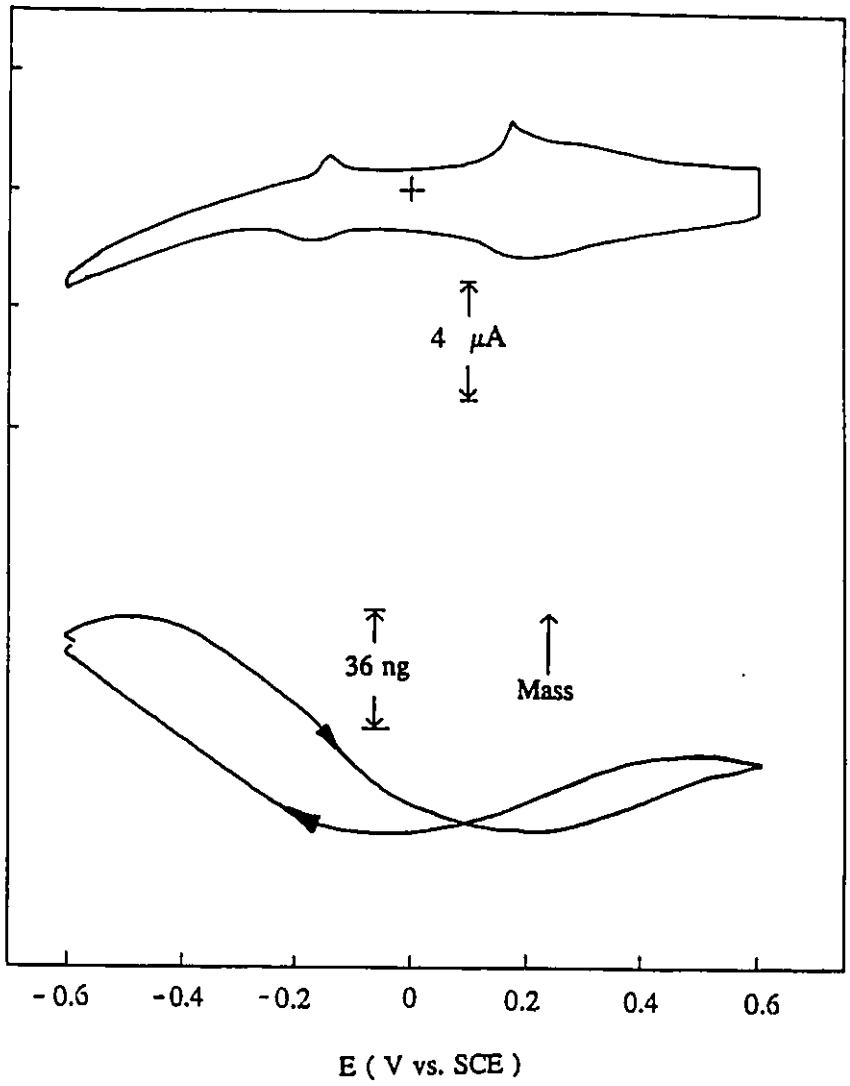

Figure 25. A cyclic voltammogram and mass response of the double layer region of potential for the EQCM gold electrode in 0.1 M $KClO_4$/0.02 M phosphate buffer (pH = 7.0). Scan rate = 20 mV/s.

electrode of an RRDE. Adzic et. al.[63] observed similar small peaks in the potential range between -0.4 and +0.6 V vs. SCE. on different single crystal faces of gold ((100), (110) and (111)) in 0.1 M NaOH/0.038 M phosphate buffer solution (pH = 7.4). These peaks changed in position and shape with the different faces and were suggested to be due to the formation of the $Au(OH)^{(1-\lambda)-}$ layer, a precursor of oxide formation rather than a result of phosphate adsorption. They proposed the following mechanism for this:

$$Au + H_2O \rightarrow AuOH^{(1-\lambda)-} + H^+ + \lambda e- \qquad (4.14)$$

$$Au + OH^- \rightarrow AuOH^{(1-\lambda)-} + \lambda e- \qquad (4.15)$$

However they stated that in comparison with the process in 0.1 M NaOH solution, the peaks did not shift by the expected amount if the difference in pH was considered and indicated that further work was necessary to identify the peaks. If the peaks are a result of formation of the $Au(OH)^{(1-\lambda)-}$, there should be two couples of small peaks in 0.1 M $KClO_4$ solution at the same potential. Our experiments in 0.1 M $KClO_4$ (Figure 20) did not reveal two pairs of small current peaks at ca. -0.2 V and 0.2 V, and in addition, the differential capacitance results indicate only that there is only a weak adsorption of perchlorate ions on the gold electrode. The difference between CVs in 0.1 M $KClO_4$ and 0.1 M $KClO_4$/0.02 M phosphate buffer solutions indicates that it is the phosphate ions which interact with the gold electrode surface. The evidence to verify this view can be

seen from the experiments described below.

In order to understand what causes these small current peaks in phosphate buffer solution, concentrated phosphate was added into 0.1 M $KClO_4$ solution in our experiments. It was found these peaks appeared even when the concentration of phosphate in the bulk solution was 1 x 10^{-4} M. The peaks were observed for all electrodes and three different samples of phosphate were used, so they are unlikely to be a result of impurities in the solutions. Hence, it is suggested that phosphate ions are adsorbed at the gold electrode surface in the double layer region.

In a phosphate buffer solution (pH = 7.0), the possible states of phosphate in aqueous solution are $H_2PO_4^-$, HPO_4^{2-}, PO_4^{3-} ions and molecular H_3PO_4, according to the following dissociation equilibria[64]:

$$H_2PO_4^- = HPO_4^{2-} + H^+ \qquad K_1 = 10^{-7.2} \qquad (4.16)$$

$$HPO_4^{2-} = PO_4^{3-} + H^+ \qquad K_2 = 10^{-12.3} \qquad (4.17)$$

$$HPO_4^{2-} + H_2O = H_2PO_4^- + OH^- \qquad K_2' = 10^{-6.8} \qquad (4.18)$$

$$H_2PO_4^- + H_2O = H_3PO_4 + OH^- \qquad K_1' = 10^{-11.85} \qquad (4.19)$$

where K_1, K_2 are the respective dissociation constants at room temperature and K_1', K_2' are respective hydrolysis constants. Since the K_2 and K_1' are very low, the presence of PO_4^{3-} and H_3PO_4 in solution may be negligible. It can be calculated that the dominant

species of phosphate buffer at pH = 7.0 are $H_2PO_4^-$ (about 61%) and HPO_4^{2-} (about 39%).

The results of our differential capacitance experiments (Figure 26) in 0.1 M $KClO_4$ with different concentrations of phosphate solution show a substantial increase in capacitance with the addition of phosphate so that at 0.02 M phosphate two peaks are visible at ca. - 0.2 V and +0.2 V. The differential capacitance peaks at ca. -0.2 V and 0.2 V increase with the increasing of the concentration of phosphate. These results strongly suggest specific adsorption of phosphate ions perhaps with some charge transfer. A similar large increase in capacity has recently been observed by Ross and D'Agostino[65] when H_2SO_4 was added to 0.01 M $HClO_4$ at gold single crystals. Like the phosphate ion HSO_4^- has a more extensive specific adsorption than ClO_4^-. However our differential capacitance results do not agree with those of Hill et. al.[38, 39] In similar solutions these authors found a maximum value of around 30 $\mu F/cm^2$, a similar value to that seen in solutions of 0.1 M $KClO_4$ alone. The reason for this difference is not known but two possibilities may be a different method of preparation of the gold electrode or the presence of other ions perhaps Cl^- from concentrated HCl used to adjust the pH of the buffer. The method of buffer preparation was not described by Hill[38] et. al., but in our experiments HCl was not used to adjust pH. From our experiment it seems that the phosphate adsorption occurs at about -0.15 and 0.2 V. Comparing these curves (Figure 26), it is observed that the two peaks at -0.16 V and 0.23 V at differential capacitance-potential curves are associated with the adsorption of phosphate species. From the voltammogram of EQCM gold electrode in phosphate buffer, we estimate the charge involved in the two

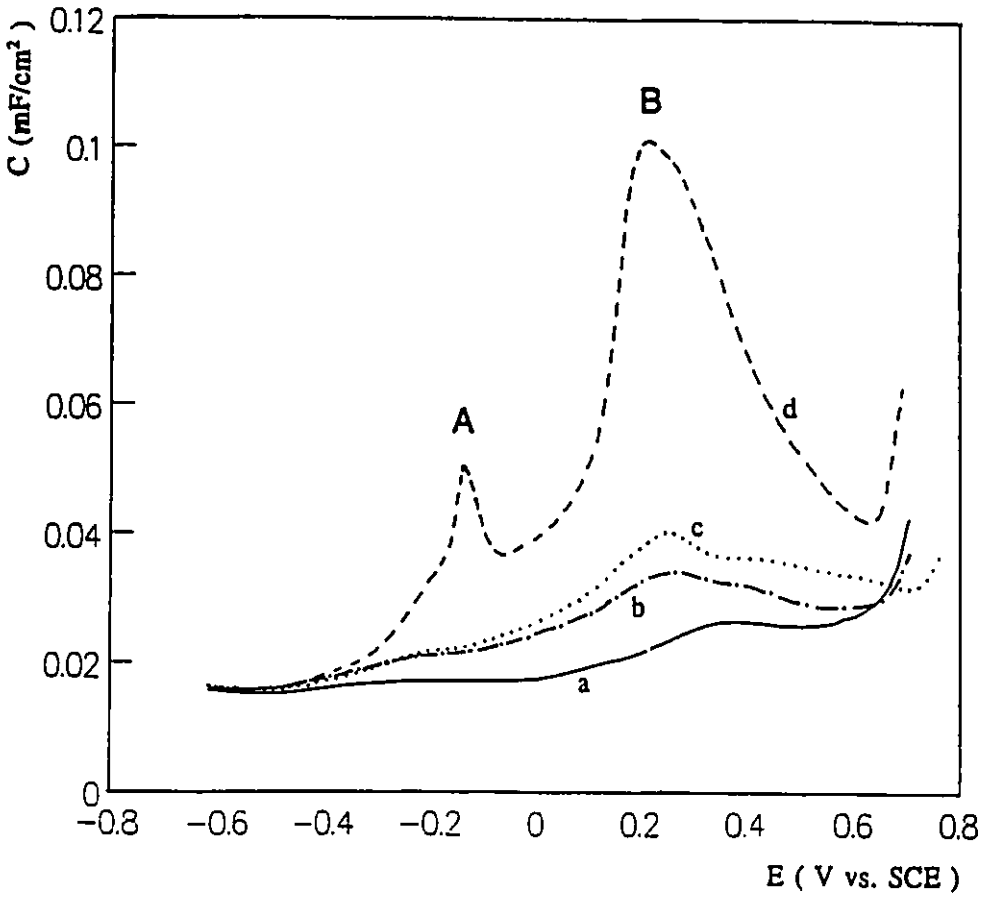

Figure 26. Differential capacitance-potential curves of the EQCM gold electrode in (a) 0, (b) 1 x 10^{-4} M, (c) 1 x 10^{-3} M, (d) 1 x 10^{-3} M, (e) 0.02 M phosphate with 0.1 M $KClO_4$ solution. Scan rate = 20mV/s, frequency = 16 kHz.

pairs of small peaks is about 20 μC which would lead very small mass change.

The effect of increasing amounts of phosphate ions in the electrolyte on the mass response was also investigated. Figure 27 shows the mass response between -0.6 V and 0.6 V at different concentrations of phosphate in 0.1 M $KClO_4$ solution. From the mass responses, it can be distinguished that at potentials above 0 V an increase in concentration of phosphate causes a gradual increase in mass as potential is increased. A similar effect was observed when the potential was cycled between -0.6 V to 1.2 V (Figure 28). This increase may correspond to the increased adsorption of phosphate species at the electrode surface as the electrode potential becomes more positive. The mass increase at potentials below 0 V shows little change with phosphate concentration, this region will be discussed later.

All the information above indicates that phosphate species have an influence on the surface of the gold electrode in the double layer region of potential especially at ca. -0.16 V and ca. 0.2 V in 0.1 M $KClO_4$ solution.

4.5.3. The Behaviour of Gold Electrode in Phosphate Buffer Solution - Oxidation and Reduction of the Electrode Surface

A cyclic voltammogram and typical mass response obtained from a deposited EQCM gold electrode in 0.02 M phosphate buffer with 0.1 M $KClO_4$ solution (pH = 7.0)

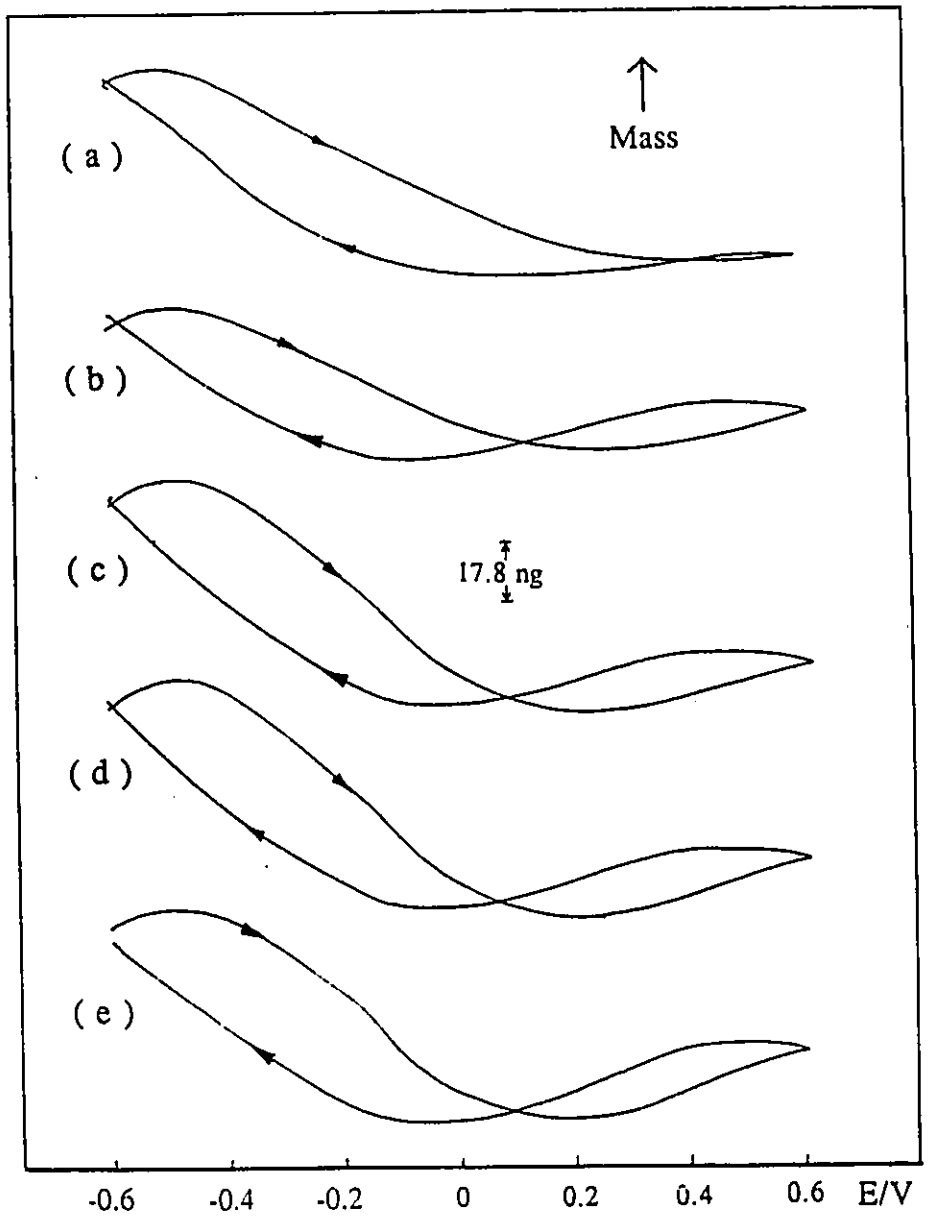

Figure 27. The mass responses of the EQCM gold electrode in (a) 0, (b) 1 x 10^{-4} M, (c) 1 x 10^{-3} M, (d) 1 x 10^{-2} M, (e) 0.02 M phosphate with 0.1 M $KClO_4$ solution in double layer region of potential. Scan rate = 20 mV/sec.

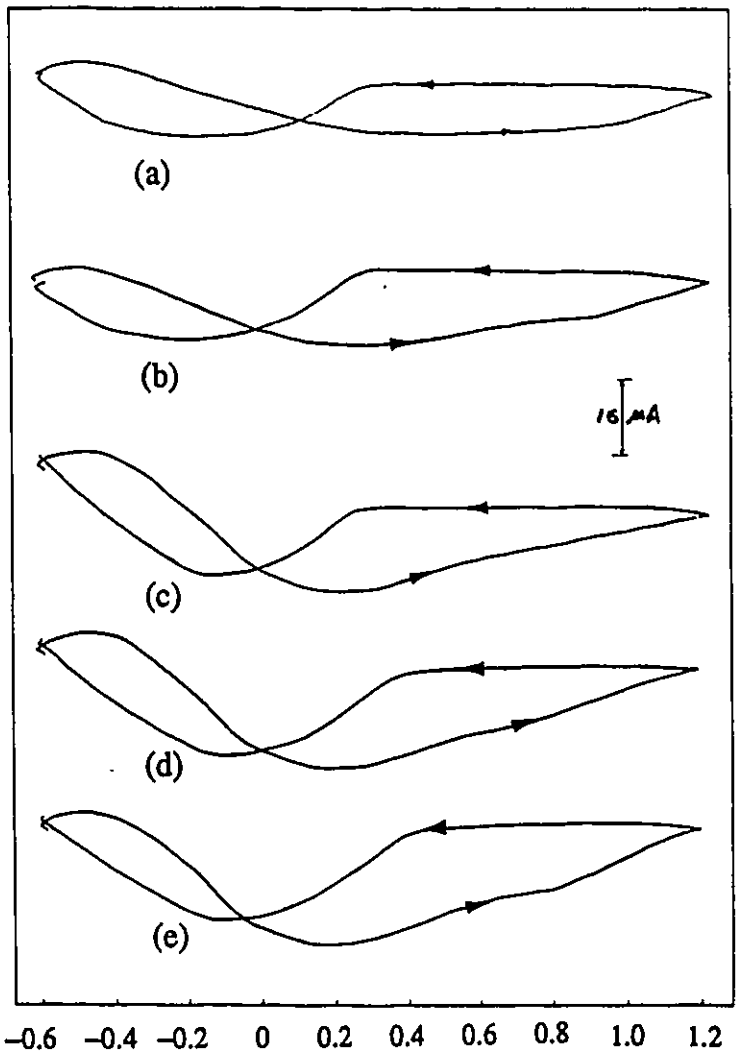

Figure 28. The mass response of the EQCM gold electrode in (a) 0, (b) 1 x 10^{-4} M, (c) 1 x 10^{-3} M, (d) 1 x 10^{-2} M, (e) 0.02 M phosphate with 0.1 M $KClO_4$ solution from -0.6 to 1.2 V. Scan rate = 20 mV/sec.

is shown in Figure 29. The three discernible peaks in the region of surface oxidation are characteristic of polycrystalline gold electrodes in a variety of solutions. Their distribution depends on the nature of the anion and on electrode pre-treatment and aging effects as described by Florit et. al.[62]

A typical mass response that accompanies the voltammogram of the EQCM gold electrode in 0.1 M $KClO_4$/0.02 M phosphate buffer (Figure 29) shows several features.

a) A steady increase in mass as the potential is scanned positive from ca. 0 V, this is most likely to be a result of increased adsorption of both phosphate and perchlorate ions (a similar but smaller mass increase in the double layer region of potential was observed for Au in 0.1 M $HClO_4$ solution but not in 1 x 10^{-3} M $HClO_4$ solution (see Figure 18 and Figure 19)).

b) An unusual increase in mass as the electrode potential is taken to potentials more negative than -0.2 V (this was also observed in 0.1 M $KClO_4$ solution and in phosphate solutions as shown in Figures 20 and 25).

c) The oxidation of the gold surface at potentials larger than 0.7 V can be distinguished from the mass response but the gold oxide reduction process cannot be distinguished from the mass decrease on the reverse scan. The mass response of Figure 29 shows no difference in mass between beginning and end of the cycle and this result may be obtained reproducibly. In addition, as seen in previous figures, there is an "isomass" point at about -0.17 V where the mass of the electrode passes through the same point on the forward and reverse scans with the mass increasing on either side of this

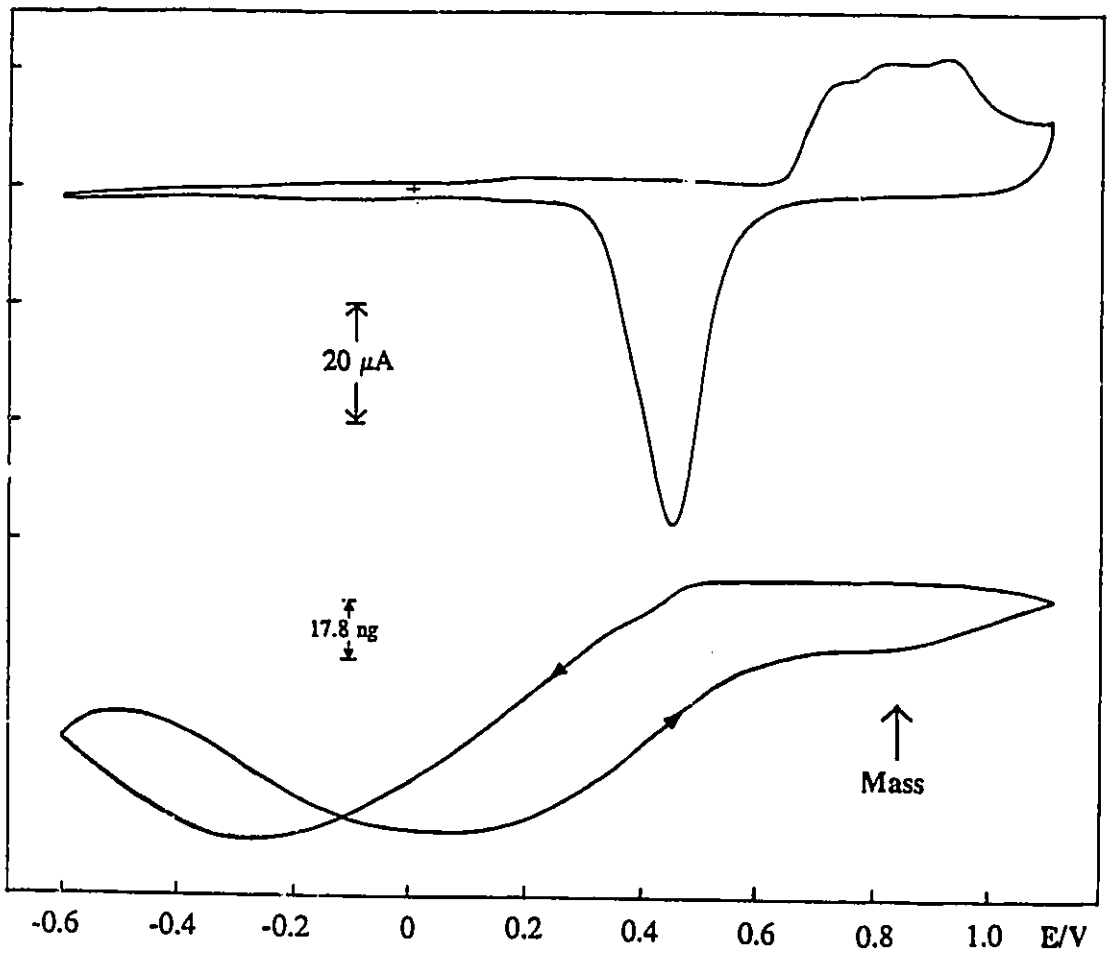

Figure 29. A cyclic voltammogram and mass response for the EQCM gold electrode in 0.1 M $KClO_4$/0.02 M phosphate buffer (pH = 7.0). Scan rate = 20 mV/s.

point.

Ring-disc experiments were also performed to investigate the possibility of gold dissolution during complete voltage cycles in phosphate buffer. Cadle and Bruckenstein[66] observed gold dissolution during the reduction of gold oxide films in acid media from a ring-disc electrode. They concluded that the quantity of this cathodically dissolved gold was a function of the electrode rotation speed, and the amount of gold oxide reduced. In order to examine the extent of dissolution of gold in neutral media, we performed rotating ring-disc electrode experiments in 0.1 M phosphate buffer. Figure 30 shows a disc current-potential curve and the corresponding ring current-potential curve obtained at the gold ring-gold disc electrode in 0.1 M phosphate buffer (pH = 6.0) solution. The ring potential was controlled at 0.0 V vs. S.C.E. Corresponding to the gold oxide reduction peak, there is a ring current peak from the i_R-E_D curve. This current peak was caused by the reduction of a small quantity of a soluble gold species produced during the reduction of the gold oxide at the disc. The faster the rotation speed was, the larger the ring current peak was, i.e. the quantity of this cathodically dissolved gold was a function of the electrode rotation speed. The amount of the soluble gold species detected by the ring electrode at ω = 25 Hz is (7.4×10^{-12}/n) mol (calculated from the charge, n is the number of electrons transferred during the electrochemical reaction) which is only 0.31% of the total oxidation charge. If the (7.4×10^{-12}/n) mol is caused by gold reduction, the mass of gold lost from the electrode would be 7.2×10^{-10} g i.e. 0.72 ng which is too small to detect by using the electrochemical quartz crystal microbalance. In

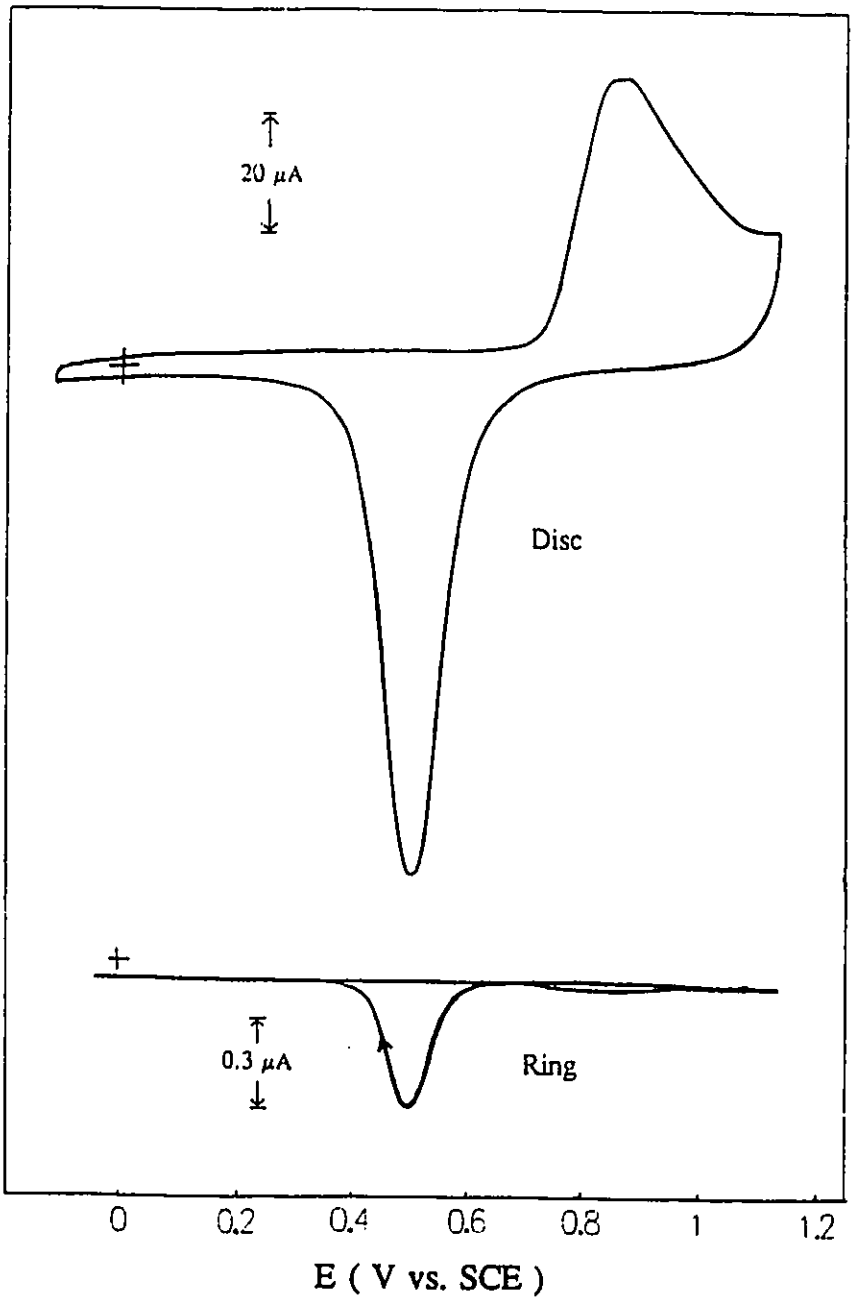

Figure 30. Current-potential curves in 0.1 M phosphate buffer at a gold ring-gold disc electrode. ω = 25 Hz, Scan rate = 50 mV/s.

addition this amount would probably be lower at a stationary electrode. This is why no difference is found in mass between beginning and end of a scan (figure 29).

4.5.4. Summary

i) Two pairs of current peaks are observed in cyclic voltammograms of the double layer region of potential (Figure 25).

ii) Differential capacitance results indicate that these peaks result from adsorption and partial discharge of phosphate species.

iii) Increased amounts of phosphate species in the electrolyte lead to increases in mass observed at potentials greater than the E_{pzc}.

iv) In phosphate buffer solution mass responses are stable with successive oxidation/reduction cycles unlike the results in $HClO_4$ solutions where mass response are unstable due to larger amounts of dissolution of gold on cycling.

4.6. Adsorption of 4,4'-Bipyridyl at the EQCM Gold Electrode

4.6.1. Electrode Response with Adsorbed 4,4'-bipyridyl

For some systems (iodide at platinum[67] and dopamine at silver[68]) it is possible to observe adsorption simply through the instantaneous mass change seen when a

concentrated solution of the compound of interest is injected into the electrolyte with the electrode poised at constant potential. Our results show that this does not appear to be the case for 4,4'-bipyridyl. There is a negligible instantaneous change after addition of an aliquot of 4,4'-bipyridyl solution (to give a final concentration of 0.1 mM) to the background electrolyte. However, the mass does change gradually (by about 150 ng) over longer periods of time. These observations are true whether the experiment is carried out at open circuit (after reduction of the electrode surface) or at a constant potential of -0.1 V. Thus adsorption of 4,4'-bipyridyl seems to be a slow process.

Because of the slow adsorption, experiments with 4,4'-bipyridyl were carried out (after obtaining a stable mass response in buffer) by using a bulk electrolyte containing 0.1 mM, 0.5 mM or 5 mM 4,4'-bipyridyl and allowing adsorption (with the electrode poised at open circuit) for ca. half an hour. The electrode potential was then cycled between - 0.6 V and 0.6 V with 4,4'-bipyridyl remaining in the electrolyte. (The chosen potential range spans that for cytochrome c electrochemistry (-200 mV to +200 mV) and at the same time avoids any oxidation of the electrode surface and the consequent restructuring of the electrode resulting from place exchange[5, 69]). There is little change in the cyclic voltammogram upon adsorption of the 4,4'-bipyridyl. However, when the current is recorded on an expanded scale (Figure 31) the double layer charging current is seen to be much reduced by the presence of 4,4'-bipyridyl and the peaks at -0.16 V in 0.1 M $KClO_4$/0.02 M phosphate are removed. Although the peaks at positive potentials (ca. 0.2 V in buffer) had not disappeared, they shifted positively to ca. 0.4 V. (Figure 31). The

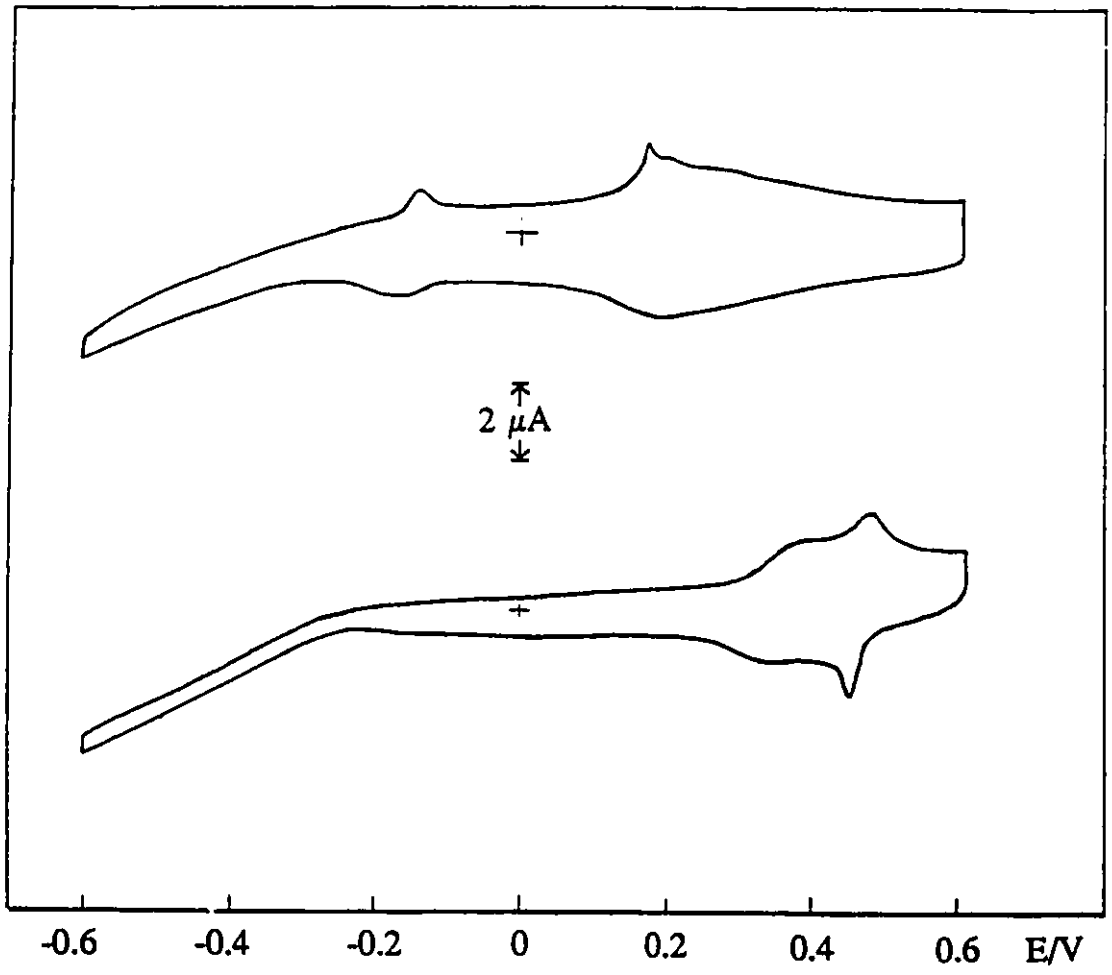

Figure 31. Cyclic voltammogram for an EQCM gold electrode in 0.1 M $KClO_4$/0.02 M phosphate solution with no Bipy (upper curve) and after adsorption of 0.5 mM 4,4'-bipyridyl for 30 minutes at open circuit (lower curve). Scan rate = 20 mV/s. The lower curve was recorded in the electrolyte containing 0.5 mM Bipy.

shape of cyclic voltammograms for the background electrolyte containing 0.1 mM, 0.5 mM, 5 mM in the double layer region of potential are almost the same, the only difference is that there is a small potential shift of the current peaks at ca. 0.4 V. The reduction in charging current is expected if ions that are specifically adsorbed at the interface are replaced by the neutral 4,4'-bipyridyl molecule. This picture is confirmed by separate differential capacitance experiments (Figure 32) which showed the expected substantial reduction in the interfacial charge after adsorption of 4,4'-bipyridyl and replacement of adsorbed anions with neutral organic molecules. Figure 32 indicates that adsorption of 4,4'-bipyridyl leads to removal of the capacitance peaks due to phosphate adsorption as well as a reduction in the capacitance to values lower than those observed in 0.1 M $KClO_4$ (Figure 21). The capacitance peak at about 0.5 V for 0.5 mM bipyridyl corresponds to the peaks seen in the cyclic voltammogram (Figure 31). The differential capacitance results shown here are qualitatively similar to those reported earlier by Hill and Uosaki[38] who also observed a decrease in capacitance after adsorption. However, as described earlier, they did not observe the large peaks attributed to phosphate adsorption in their background response.

The capacitance peak at about 0.5 V (curve c in Figure 32) and the peaks in the voltammogram (lower curve in Figure 31) indicate that at more positive potentials some bipyridyl may be removed from the surface and replaced by phosphate species. This is understandable since the neutral organic adsorbate is less able to compete with anions as the potential moves further away from the potential of zero charge in a positive direction.

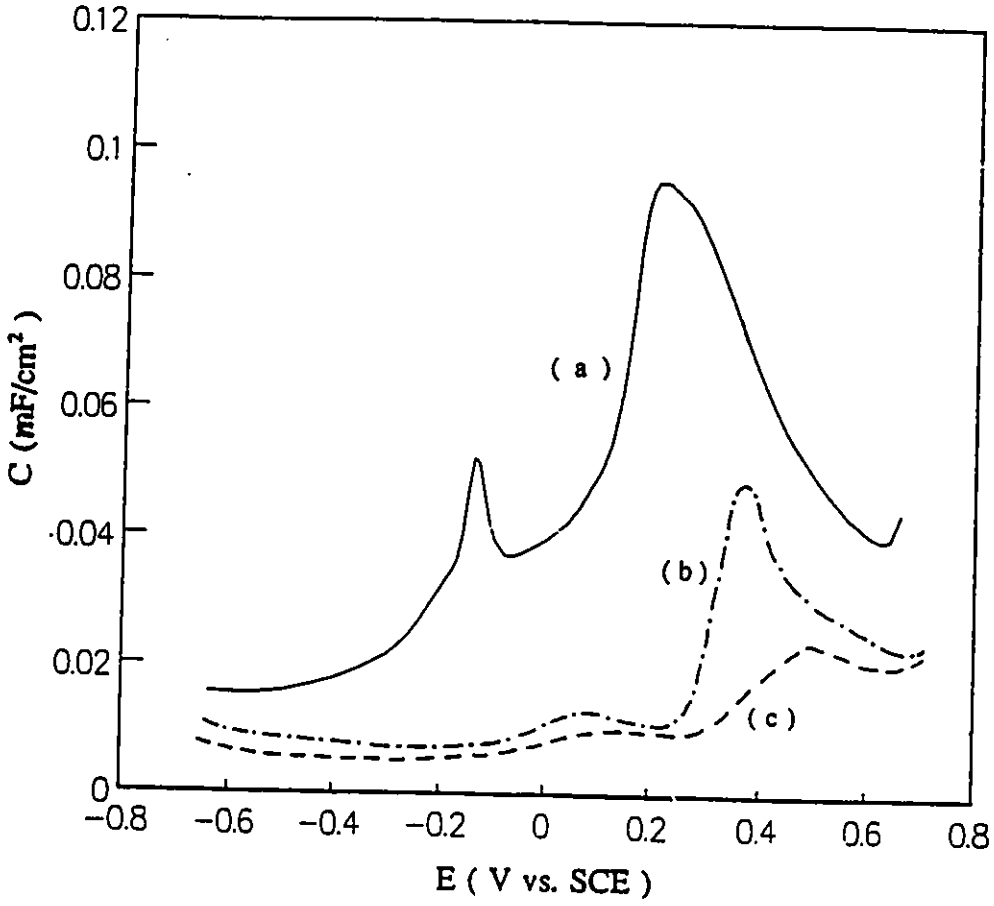

Figure 32. Differential capacitance-potential curves of the EQCM gold electrode in 0.1 M $KClO_4$/0.02 M phosphate solution containing (a) 0, (b) 0.1 mM, (c) 0.5 mM 4,4'-bipyridyl. Scan rate = 20 mV/s. Frequency = 16 Hz.

These results show that the 4,4'-bipyridyl molecules can not replace adsorbed phosphate completely when the bulk concentration of bipyridyl is 0.5 mM. There seems to be some competition between adsorbed 4,4'-bipyridyl and adsorbed phosphate ions:

$$Au(H_2O)_{ads} + A^- \rightleftharpoons Au(H_2O)_{ads}(A^-)_{ads} \quad (4.20)$$

$$Au(H_2O)_{ads} + Bipy \rightleftharpoons Au(H_2O)_{ads}(Bipy)_{ads} \quad (4.21)$$

$$Au(H_2O)_{ads}(Bipy)_{ads} + A^- \rightleftharpoons Au(H_2O)_{ads}(A^-)_{ads} + Bipy \quad (4.22)$$

While the changes in the cyclic voltammogram as a result of the adsorption of 4,4'-bipyridyl are subtle, a dramatic change occurs in the mass response. The presence of adsorbed 4,4'-bipyridyl gives rise to a mass response which is flat over a potential range of 1.2 V. A typical response is shown in Figure 33 where the behaviour in the absence of 4,4'-bipyridyl is also given for comparison. The mass response in the presence of 4,4'-bipyridyl is extremely reproducible upon repetitive cycling, and the fact that it is largely unchanged in the presence of 4,4'-bipyridyl (in contrast to the result in buffer) reinforces the view that the molecule is absorbed over the whole potential range scanned, in agreement with previous observations[38, 39] and with differential capacitance results. The stability of the response after adsorption indicates either that 4,4'-bipyridyl is not lost from the electrode surface upon cycling over this potential range, or that any 4,4'-bipyridyl lost is replaced by adsorption of 4,4'-bipyridyl from solution. The behaviour of the electrode

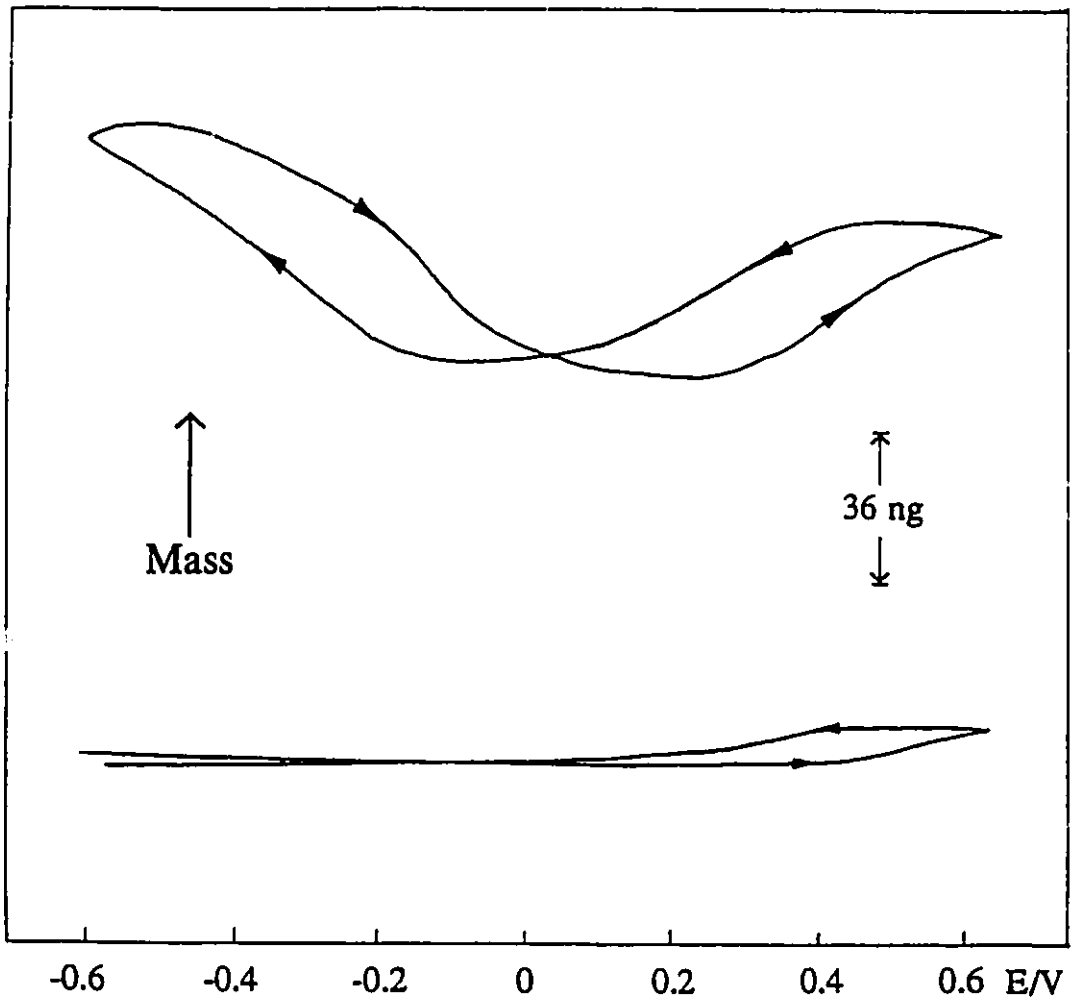

Figure 33. Mass responses for an EQCM gold electrode in 0.1 M $KClO_4$/0.02 M phosphate buffer with no Bipy (upper curve) and after adsorption of 5 mM 4,4'-bipyridyl for 30 minutes at open circuit (lower curve). Scan rate = 20 mV/s. The lower curve was recorded in the electrolyte containing 5 mM Bipy.

after rinsing in phosphate buffer (see below) perhaps indicates that the latter case is more appropriate. There is some hysteresis in the mass response at the more positive potentials and this may result from some phosphate species replacing adsorbed bipyridyl, but it should be noted that the bipyridyl concentration here is 10 times larger than for Figure 32 (c).

Finally in this section we consider the orientation of 4,4'-bipyridyl on the electrode surface. Uosaki and Hill[38] observed a peak around 0 V vs. S.C.E. in the differential capacitance and proposed that this resulted from the adsorbed 4,4'-bipyridyl undergoing a transition between two different orientations (Figure 34). The differential capacitance experiments shown in Figure 32 reveal a similar very small peak at 0.1 V vs. SCE which may arise from the orientation of 4,4'-bipyridyl on the electrode surface. However, a re-orientation of 4,4'-bipyridyl, if present, does not appear to be indicated in the mass response. There are small changes in the mass and a slight hysteresis in the potential range of interest (ca. 0.1 V) but these are at the limit of sensitivity of the EQCM and therefore cannot interpreted easily. It is questionable whether in fact a reorientation would be observable in the mass response, although a reorientation leading to a significant change in packing density should in principle be visible.

4.6.2. Strength of Adsorption of 4,4'-Bipyridyl

In studies of promoter/cytochrome c systems, the pre-adsorption of the promoter

(A)

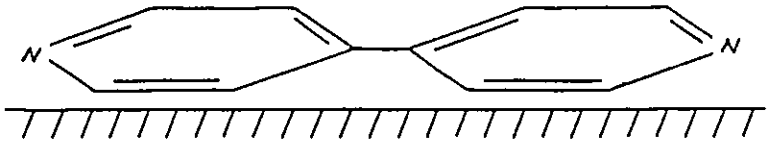

(B)

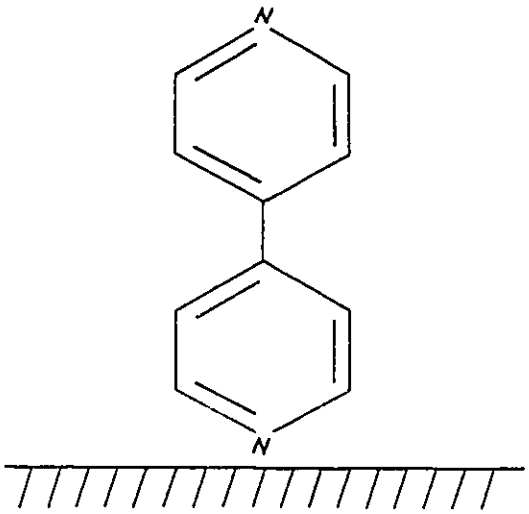

Figure 34. Two orientations of 4,4'-bipyridyl adsorption at gold electrode surface. (A) parallel, (B) vertical.

followed by rinsing is a fairly common technique of electrode preparation. Some simple experiments were carried out to investigate the strength of the 4,4'-bipyridyl adsorption and the effect of rinsing an electrode on which 4,4'-bipyridyl had been preadsorbed. The procedure yielding the response shown in Figure 33 was repeated and then the electrolyte containing 4,4'-bipyridyl removed from the cell and replaced with fresh phosphate buffer. Figure 35 shows a typical voltammogram and the mass responses accompanying the first, third and fifth voltammograms obtained after such an electrolyte replacement procedure. Even on the first cycle, it is clear from the mass response (which is intermediate between those of Figure 33 before and after adsorption of 4,4'-bipyridyl) that some 4,4'-bipyridyl has been lost as a result of the rinsing procedure and further losses are visible as the cycling continues and the mass response tends towards that seen in the absence of 4,4'-bipyridyl. It is also noticeable that the isomass point (indicated by the arrow) seems to have been shifted to more negative potentials relative to its value in buffer and this trend is reversed upon cycling as 4,4'-bipyridyl is removed from the electrode surface. The increase in mass at potentials more negative than the isomass point is also re-established, but the mass change of the electrode after rinsing the adsorbed 4,4'-bipyridyl in phosphate buffer is not the same as it was before adsorption of 4,4'-bipyridyl (Figure 33). Thus the act of rinsing the electrode with buffer can remove most of the adsorbed 4,4'-bipyridyl, and this removal process is accelerated by potential cycling after rinsing. Under the cycling, it seems the adsorbed 4,4'-bipyridyl can be removed from the electrode completely (the cyclic voltammogram and the mass change after more than twenty cycles

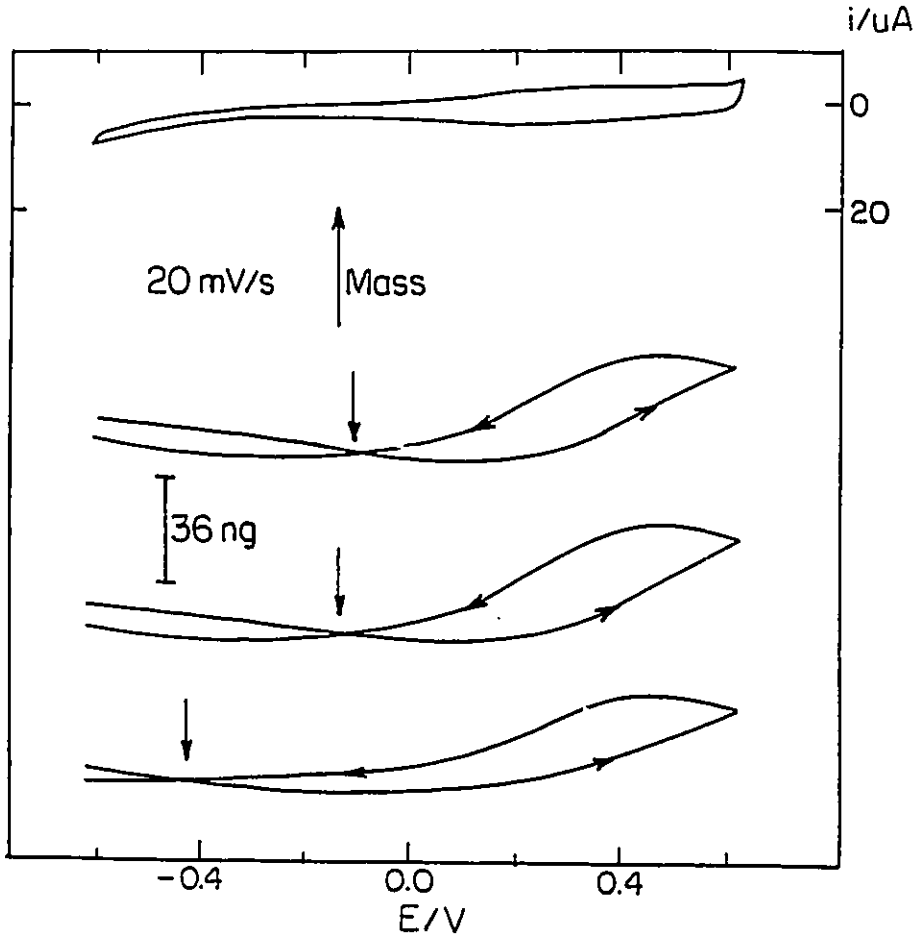

Figure 35. Typical cyclic voltammogram (top) , and the mass responses that accompany the first (lowest), third (middle) and fifth (upper) voltammograms after replacement of a 5 mM Bipy containing electrolyte with fresh phosphate buffer. Scan rate = 20 mV/s. The mass responses are displaced along the vertical axis for clarity.

are almost the same as they were before the adsorption of 4,4'-bipyridyl in buffer solution). These results demonstrate that the mass response provides a simple and more dramatic picture of the changes in adsorption occurring at the electrode than the cyclic voltammetry which (over the potential range examined) consists largely of a small double layer charging current.

4.6.3. Effect of Oxidation/Reduction Cycles on the Adsorption of 4,4'-Bipyridyl

Further experiments were carried out with 4,4'-bipyridyl by allowing a longer time of adsorption and by extending the anodic scan limit so that the electrode surface would be oxidised and reduced in the presence of 4,4'-bipyridyl. Figure 36 shows the results obtained after allowing the electrode to be in contact with a 5 mM solution of 4,4'-bipyridyl for one hour at open circuit. The first (and subsequent) potential cycles towards the upper scan limit of 1.1 V show that the onset of surface oxidation of the gold is shifted by ca. 100 mV to a more positive potential of 0.72 V by the presence of adsorbed bipyridyl. The oxidation region becomes one sharp peak in contrast to the broad region with three small peaks that is seen in the absence of 4,4'-bipyridyl (Figure 29). The mass response of the EQCM gold electrode for the anodic scan is very different from that in Figure 29. It is largely constant over almost the entire potential range except for a small increase as the surface is oxidised. This increase is only a small fraction of that to be expected from a simple picture of addition of a layer of oxide to the electrode.

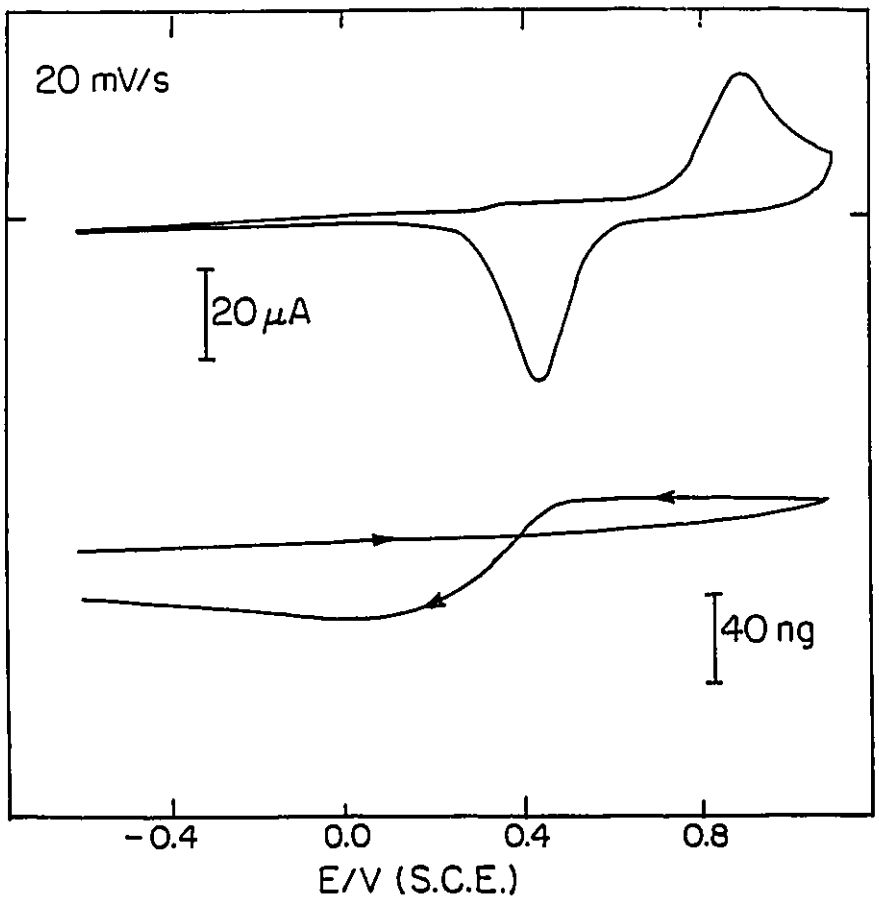

Figure 36. Cyclic voltammogram and mass response for gold electrode after immersion in an electrolyte containing 5 mM Bipy for 1 hour (at open circuit). Response recorded with 5 mM Bipy still in the electrolyte at a scan of 20 mV/s.

We suggested above that there seems to be a small fraction of the electrode surface covered with phosphate species. This part of the gold electrode covered by phosphate ions ($Au\text{-}A^-$) can be oxidised to gold oxide, followed by the place-exchange:

$$Au\text{-}A^- + H_2O \longrightarrow Au\text{-}OH + H^+ + A^- + e^- \qquad (4.23)$$

$$Au\text{-}OH \longrightarrow Au{=}O + H^+ + e^- \qquad (4.24)$$

$$Au{=}O \longrightarrow O{=}Au \qquad (4.25)$$

After (4.25) water or perhaps bipyridyl may then adsorb, but since only a small amount of $O{=}Au\text{-}H_2O$ or O=Au-Bipy is formed, the mass does not increase very much. The remainder of the gold electrode surface is covered by adsorbed 4,4'-bipyridyl before oxidation, we suggest that the gold surface covered by 4,4'-bipyridyl may also be oxidised, i.e.

$$Au(H_2O)_{ads}(Bipy)_{ads} \longrightarrow O{=}Au(Bipy)_{ads} + 2H^+ + e^- \qquad (4.26)$$

This equation represents a situation where on an unoxidised surface, the bipyridyl is adsorbed along with water as has been suggested by other workers[49], whereas when the surface is oxidised bipyridyl is adsorbed on the gold itself. This would lead to a situation

where the effective mass change for this process in Equation (4.26) is simply the loss of two protons. The combination of processes occurring (equations 4.23 to 4.26) results in a small overall mass increase. However these equations are only one possible explanation for the observed results.

The major feature of the cathodic scan is a sharp decrease in mass coincident with the oxide reduction process and thereafter a small increase in mass is seen. If the potential is held at the negative scan limit, there is a further small increase in mass but it is insufficient to bring the mass up to its initial value. Thus the mass at the end of a scan is less than it was at the beginning. Further information on the processes occurring at the electrode surface upon oxidation may be obtained by consideration of the experiment shown in Figure 37, where after 4,4'-bipyridyl was adsorbed overnight at open circuit and with a bulk concentration of 5 mM the potential was cycled from the negative limit of -0.7 V to successively increasing upper limits. The cyclic voltammetry shows that provided the potential is restricted to values below ca. 0.78 V (curve 3 of Figure 37) there is no decrease in mass on the cathodic scan. Under these conditions the oxidation process occurring appears to be reversible and may correspond to the initial development of the oxide on gold[69] where place exchange does not occur. As the extent of oxidation of the surface increases, the familiar oxide reduction peak becomes visible indicating the onset of irreversible surface oxidation. This is a result of the place exchange process where the oxide ion moves below the uppermost layer of gold atoms and is effectively inserted into the lattice[5, 69]. It is only when the potential is taken to a value sufficiently positive for

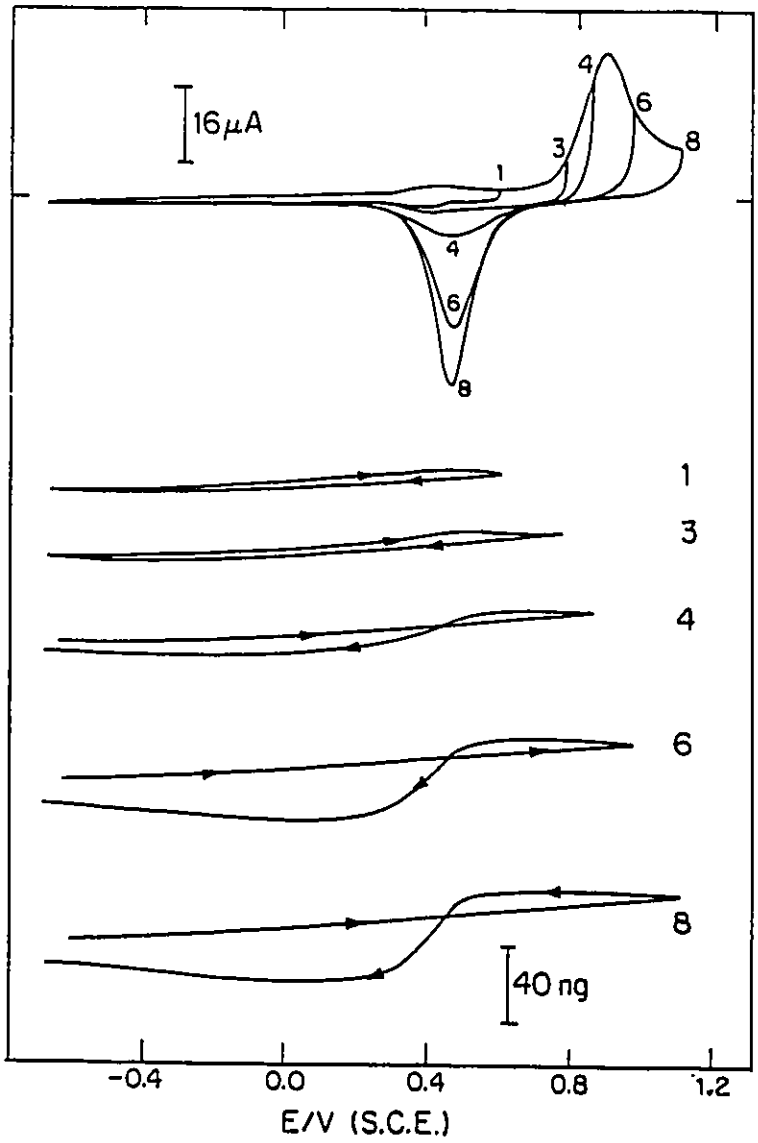

Figure 37. Cyclic voltammogram and mass responses for a gold electrode after being exposed to a 5 mM solution of Bipy overnight. The anodic potential limit was taken to successively more positive potentials for 8 cycles. Some cycles are omitted for clarity. Mass responses are offset from each other for the same reason and results were obtained with 5 mM Bipy remaining in the electrolyte. Scan rate = 20 mV/s.

place exchange to occur that the loss in mass on the cathodic scan appears. As Figure 37 shows (scans 4, 6 and 8), this mass loss becomes larger as the extent of oxidation (and hence the size of the oxide reduction current) increases.

Figure 37 indicates that the decrease in mass (see Figure 36) is a consequence of the reversal of the place exchange process (i.e. the reverse of equation (4.3)). There is a small increase in mass as the potential proceeds towards the negative limit and if the potential is held at the limit a further small increase is registered but the sum of these two increases is not sufficient to return the mass to its value at the start of the cycle. Thus a complete cycle results in a net mass loss and further cycling results in further net mass losses. The mass decrease occurring on the cathodic scan is greater than the small increase seen on the anodic scan and so is not simply a reversal of the processes described above. The decrease is probably a composite of three contributions. First, there will be a net loss of oxide on sites not occupied by 4,4'-bipyridyl (i.e. a reversal of steps (4.1) to (4.3) shown at p.56). Second, the mass lost during the place exchange reversal and subsequently recovered when the cathodic scan continues and is held at the negative limit is indicative of a small amount of adsorbed bipyridyl being removed and then undergoing readsorption during the remainder of the cathodic scan. The final contribution is a small but permanent decrease in the mass of the electrode (note that if the electrode surface is only partially oxidised and no place exchange occurs then the mass loop closes - e.g. curves 1 and 3 of Figure 37) and could be explained by some soluble gold produced upon oxide reduction being lost into solution, perhaps as a bipyridyl complex. As mentioned

earlier, it is known that soluble gold is produced in trace amounts during reduction of gold oxide, and it also known that Ag(I) and other transition metals form complexes with 4,4'-bipyridyl[70, 71] (complexes with 2,2'-bypiridyl are of course much more common because of the bidentate nature of the ligand) although Ag(I) forms polymeric species where the 4,4'-bipyridyl acts as a bridge and ligands such as nitrate and sulphate are also coordinated. Indeed SERS experiments have indicated that such complexes form on the electrode surface after oxidation of Ag electrodes in the presence of 4,4'-bipyridyl[53, 54]. The fact that there is no net loss upon electrode cycling in phosphate buffer in the absence of 4,4'-bipyridyl (Figure 29) points to possible complex formation with 4,4'-bipyridyl.

Finally a similar experiment to that reported earlier (and shown in Figure 35) was performed to investigate the effects of an increased time of exposure to 4,4'-bipyridyl and of cycling the electrode through oxidation and reduction on the strength of adsorption. An electrode that had been exposed to a solution of 5 mM 4,4'-bipyridyl overnight was then cycled such that it yielded a mass response and voltammogram like those shown in Figure 36. The electrolyte was then changed to one of pH = 7 phosphate buffer and cyclic voltammetry and mass responses recorded. The results are shown in Figure 38. The mass response demonstrates (as was the case when the potential cycle was restricted to the range between -0.6 V and +0.6 V) that the act of changing the electrolyte is sufficient to remove some of the adsorbed 4,4'-bipyridyl. The CV and mass response are much closer to those shown in Figure 33 than those in Figure 36 and the isomass point has reappeared and shifts towards its position in the absence of 4,4'-bipyridyl as the

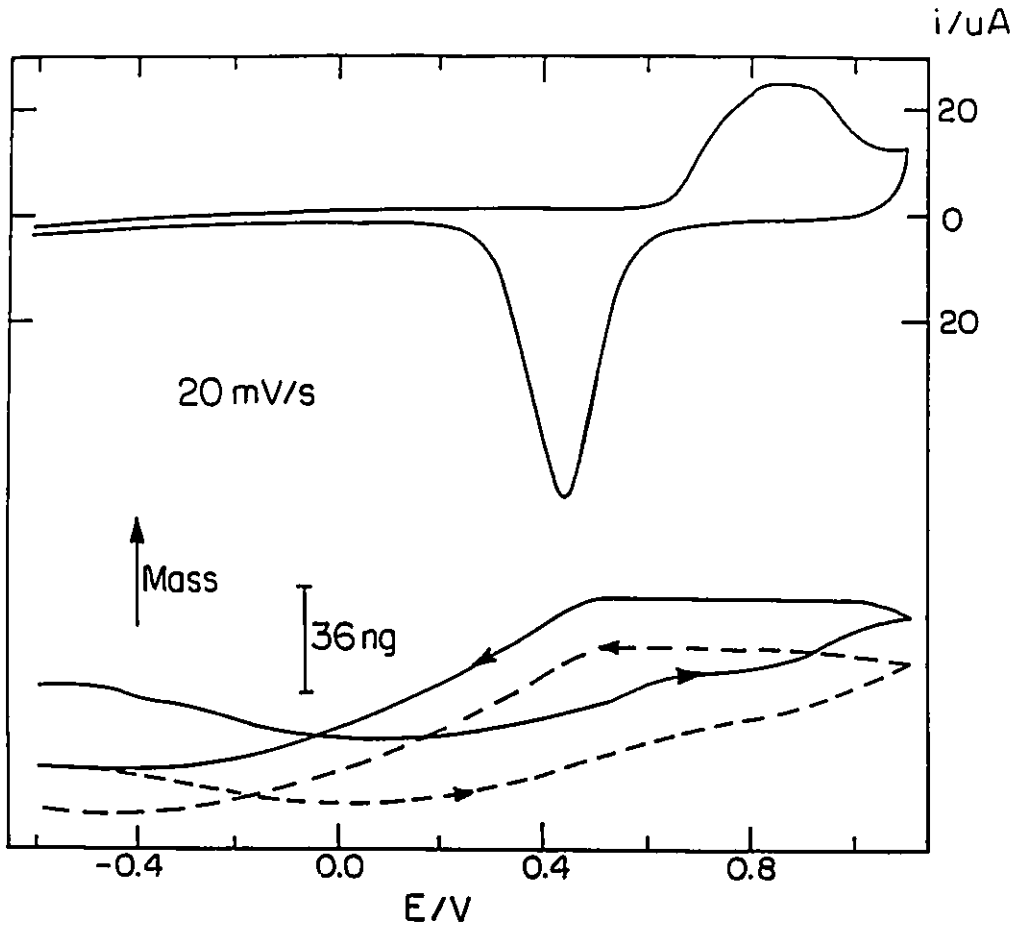

Figure 38. Cyclic voltammogram (first scan only) and mass response for gold electrode such as that of Figure 31, after replacement of 4,4'-bipyridyl containing electrolyte with fresh phosphate buffer. Solid line - Mass response accompanying the first scan, dashed line accompanying second scan.

electrode is cycled. Figure 38 also shows that cycling results in a permanent decrease in mass of the electrode as 4,4'-bipyridyl is removed from the surface. The adsorption of the 4,4'-bipyridyl is again seen to be weak, such that it can be removed from the electrode surface simply by rinsing the electrode. From a comparison of this result with that shown in Figure 35 there does not appear to be any evidence for the adsorption becoming stronger with time and there is no apparent effect of cycling through oxidation and reduction of the electrode surface on the strength of adsorption.

Finally, two points remain to be discussed. The first is the isomass point and the second is the increase in mass observed at potentials negative of the E_{pzc}.

i) Isomass point - The isomass point is observed in $KClO_4$ and phosphate buffer solutions and also in experiments like those in Figures 35 and 36 where an electrode with bipyridyl adsorbed on it was examined in a buffer solution. It is always close to the point where mass is at a minimum and so it could be thought of as an approximate representation of the E_{pzc}. At the E_{pzc} where ionic adsorption should be lowest (in the absence of any adsorbed organic species) the mass of the electrode should be at a minimum. However, for experiments in $KClO_4$ (Figure 20) where the electrode surface is not oxidised or reduced, the isomass point is at a potential that is too high e.g. 0.4 V in Figure 20 when the E_{pzc} is 0.04 V. Further work is needed to understand the causes of the isomass point.

ii) Mass increase at potentials below the E_{pzc} - Mass increases at negative potentials were observed in all electrolytes used here e.g. 0.1 M $HClO_4$(Figure 18), 0.1 M $KClO_4$

(Figure 20) and phosphate buffer (Figure 29) solutions. The increase was found to grow as the potential was made more negative and becomes much larger than the mass increase observed when the electrode surface is oxidised. It is also removed by the presence of adsorbed 4,4'-bipyridyl. Although some cation adsorption might be expected at potentials below the E_{pzc} the change seems to be too large to be explained by this phenomenon. The observed mass increases may result from a process that gives rise to a frequency change not derived from a mass change, for example a change in the hydrophobic or hydrophillic character of the electrode surface. This might change the coupling between the shear waves of the crystal and the electrolyte. As for the isomass point, further work is necessary to explain the observations.

4.7. CONCLUSION

The adsorption of bipyridyl at a gold electrode is clearly visible from mass measurements which show a reproducible and almost constant mass response in the potential range from -0.6 V to +0.6 V. Mass increases occurring either side of an isomass point in pH = 7 phosphate buffer solution are removed once 4,4'-bipyridyl is adsorbed. Both differential capacitance and mass responses show that adsorption of 4,4'-bipyridyl displaces adsorbed phosphate species from the electrode surface. If the scan limit is increased such that the electrode surface is oxidised and reduced during a cycle there is still no significant change in the mass on the anodic scan, but reduction of the irreversibly

formed oxide results in a mass loss that is only partially recovered. These observations might be explained by a mechanism where 4,4'-bipyridyl is present with adsorbed water at an electrode surface that is reduced, but 4,4'-bipyridyl alone is adsorbed once the electrode is oxidised and place exchange has occurred. Reversal of place exchange leads to loss of some adsorbed bipyridyl, although readsorption occurs as the potential is taken more negative. There is also a decrease in mass that is not recovered and probably represents the loss of small amounts of gold into solution, perhaps as a bipyridyl complex. The EQCM reveals, in this instance significant information regarding the processes occurring when a gold electrode is oxidised and reduced in the presence of 4,4'-bipyridyl and show that adsorption of 4,4'-bipyridyl is weak and it may be at least partially removed from the electrode surface by washing.

REFERENCES

1. C. Lu and A. W. Czanderna, "Applications of piezoelectric quartz crystal microbalances", Elsevier, 1984.
2. J. H. Kaufman, K. K. Kanazawa and G. B. Street, Phys. Rev. Lett., 53 (1984) 2461.
3. S. Bruckenstein and S. Swathirajan, Electrochim. Acta, 30 (1985) 851.
4. S. Bruckenstein and M. Shay, Electrochim. Acta, 30 (1985) 1295.
5. S. Bruckenstein and M. Shay, J. Electroanal. Chem.,188 (1985) 131.
6. M. R. Deakin, T. T. Li and O. R. Melroy, J. Electroanal. Chem., 243 (1988) 343.
7. G. Sauerbrey, Z. Phys., 155 (1959) 206 .
8. D. A. Buttry and M. D. Ward, Chem. Rev., 92 (1992) 1355.
9. S. J. Martin, V. E. Granstaff and G. C. Frye, Anal. Chem., 63 (1991) 2272.
10. C. Lu and O. Lewis, J. Appl. Phys., 43 (1972) 4385..
11. K. K.Kanazawa and J. G. Gordon II, Anal. Chem., 57 (1985) 1770.
12. K. K. Kanazawa and J. Gorden II, Anal. Chim. Acta, 175 (1985) 99.
13. M. Thompson, A. L. Kipling and W. C. Duncan-Hewitt, Analyst, 116 (1991) 881.
14. O. R. Melroy, K. Kanazawa, J. G. Gordon II and D. Buttry, Langmuir,

2 (1986) 697.

15. M. R. Deakin, T. T. Li and O. R. Melroy, J. Electroanal. Chem., 239 (1988) 331.
16. M. Hepel, K. Kanige and S. Bruckenstein, J. Electroanal. Chem., 266 (1989) 409.
17. C. K. Baker and J. R. Reynolds, J. Electroanal. Chem., 251 (1988) 307.
18. S. Servagent and E. Vieil, J. Electroanal. Chem., 280 (1990) 227.
19. H. E. Hager, R. D. Ruedisueli and M. E. Buehler, Corrosion, 42 (1986) 345.
20. R. Schumacher, A. Muller and W. Stockel, J. Electroanal. Chem., 219 (1987) 311.
21. R. Schumacher, J. G. Gordon and O. Melroy, J. Electroanal. Chem., 216 (1987) 127.
22. W. D. Hinsberg, C. G. Willson and K. K. Kanazawa, J. Electrochem. Soc., 133 (1986) 1448.
23. E. S. Grabbe, R. P. Buck and O. R. Melroy, J. Electroanal. Chem., 223 (1987) 67.
24. C. P. Wilde and T. Ding, J. Electroanal. Chem., 327(1992)279-290.
25. B. J. Feldman and O. R. Melroy, J. Electroanal. Chem., 234 (1987) 213.
26. J. F. Alder and J. J. McCallum, The Analyst, 108 (1983) 1169.
27. D. A. Buttry, Electroanalytical Chemistry, Vol. 17, Marcel Dekker, New York, 1991.

28. M. R. Deakin and D. A. Buttry, Analytical Chem., 61 (1989) 1147A.

29. R. E. White, J. O'M. Bockris, B. E. Conway and E. Yeager, "Comprehensive Treatise of Electrochemistry", Vol. 8, Plenum Press, New Yorrk, 1984.

30. "Instrumental Methods in Electrochemistry", Southampton Electrochemistry Group, Ellis Horwood Limited, 1985.

31. D. Pletcher, "A First Course in Electrode Processes", The Electrochemical Consultancy, Alresford Press Ltd., 1991.

32. R. Schumacher, G. Borges and K. K.Kanazawa, Surf. Sci., 163 (1985) L621.

33. S. H. Cadle and S. Bruckenstein, Anal. Chem., 46 (1974) 16.

34. S. B. Brummer and A. C. Makrides, J. Electrochem. Soc., 111 (1964) 1122.

35. V A. Vicente and S. Bruckenstein, Anal. Chem., 45 (1973) 2036.

36. E. Yeager, J. O'M. Bockris, B. E. Conway and S. Sarangapani, "Comprehensive Treatise of Electrochemistry " , Vol. 9,P. 24, Plenum Press, New York, 1984.

37. A.A.Michri, A.G.Pshchenichnikov and R.Kh.Burshtein, *Elektrokhimiya 8,* 364(1972).

38. K. Uosaki and H. A. O. Hill, J. Electroanal. Chem., 122 (1981) 321.

39. M. J. Eddowes, H. A. O. Hill and K. Uosaki, Bioelectrochemistry and Bioenergetics, 7 (1980) 527-537; J. Electroanal. Chem., 116 (1980) 527.

40. J. Clavilier et C. N. V. Huong, J. Electroanal. Chem., 80 (1977) 101.

41. C. P. Wilde, Ph. D. Thesis, 1984.

42. M. J. Eddowes and H. A. O. Hill, J. Chem. Soc. Commun., (1977) 771.

43. F. A. Armstrong, H. A. O. Hill and N. J. Walton, Acc. Chem. Res., 21 (1988) 407.

44. C. Zhou, S. Ye, J-H. Kim, T. M. Cotton, X.. Yu, J. Lu and S. Dong, J. Electroanal. Chem., 319 (1991) 71.

45. N. K. Akhmetov, R. I. Kaganovich, B. B. Damaskin and E. A. Mambetkaziev, Elektrokhimiya, 14 (1978) 1761.

46. E. A. Mambetkaziev, A. M. Shaldybaeva, V. N. Statyuk and S. I. Zhdanov, Elektrokhimiya, 11 (1975) 1750.

47. M. J. Eddowes and H. A. O. Hill, J. Am. Chem. Soc., 101 (1979) 4461.

48. K. Niwa, M. Furukawa and K. Niki, J. Electroanal. Chem., 245 (1988) 275.

49. A. Czerwinski, S. Zamponi, J. Sobkowski and R. Marassi, Electrochimica Acta., 35 (1990) 591.

50. I. Taniguchi, M. Iseki, Hiroko Yamaguchi and K. Yasukouchi, J. Electroanal. Chem., 186 (1985) 299.

51. I. Taniguchi, T. Murakami, K. Toyosawa, H. Yamaguchi and K. Yasukouchi, J. Electroanal. Chem., 131 (1982) 397.

52. Y. Gui and T. Kuwana, J. Electroanal. Chem., 222 (1987) 321.

53. T. M. Cotton and M. Vavra, Chem. Phy. Lett., 106 (1984) 491.

54. T. M. Cotton, D. Kaddi and D. Iorga, J. Am. Chem. Soc., 105 (1983) 7462.

55. C. Hinnen, C. Nguyen Van Huong, A. Rousseau and J. P. Dalbera, J.

Electroanal. Chem., 95 (1979) 131.

56. H. Angerstein-Kozlowska, B.E. Conway, A. Hamelin and L. Stoicoviciu, Electrochim. Acta, 31 (1986) 1051.

57. G. R. Mundy, R. J. Potter, P. A. Christensen and A. Hamnett, J. Electroanal. Chem., 279 (1990) 257.

58. L. Stolberg, S. Morin, J. Lipkowski and D. E. Irish, J. Electroanal. Chem., 307 (1991) 241.

59. T. Takamura and K. Takamura, J. Electroanal. Chem., 39 (1972) 478.

60. M. A. Habib and J. O'M. Bockris, J. Electrochem. Soc. 132 (1985) 108.

61. J. K. Takamura, A. Mori and F. Watanabe, J. Electroanal. Chem., 102 (1979) 109.

62. M. T. Florit, M. E. Martins and A. J. Arvia, J. Electroanal. Chem., 151 (1983) 209.

63. R. R. Adzic, M. W. Hsiao and E. B. Yeager, J. Electroanal. Chem., 260 (1989) 475.

64. D. D. Perrin, "Ionization Constants of Inorganic Acids and Bases in Aqueous Solution", Second Edition. IUPAC Chemical Data Series No. 29, Pergamon Press, New York (1982).

65. P. N. Ross and T. D'Agostino, Electrochimica Acta, 37 (1992) 615.

66. S.H. Cadle and S. Bruckenstein, Anal. Chem., 46 (1974) 16.

67. Z. Shu and S. Bruckenstein, J. Electroanal. Chem., 317 (1991) 263.

68. M. Hepel, Extended Abstract 792, 178th Electrochemical Society Meeting, Seattle, 1990.

69. H. Angerstein-Kozlowska, B. E. Conway, A. Hamelin and L. Stoicoviciu, Electrochim. Acta, 31 (1986) 1051.

70. W. J. Peard and R. T. Pflaum, J. Am. Chem. Soc., 80 (1985) 1593.

71. I. S. Ahuja, R. Sing and C. P. Rai, J. Inorg. Nucl. Chem., 40 (1978) 924.

72. Cl. Buess-Herman, N. Vanlaethem-Meuree, E. Quarin and L. Gierst, J. Electroanal. Chem., 123 (1981) 21.

73. L. Stolberg, J. Richer, J. Lipkowski and D. E. Irish, J. Electroanal. Chem., 207 (1986) 213.

Appendix

For a simple resistance-capacitance (R-C) equivalent circuit in series, the impedance, Z, for the above circuit, is

$$Z=R+\frac{1}{j\omega C} \tag{A.1}$$

or

$$Z=R-\frac{1}{\omega C}j \tag{A.2}$$

where $j = (-1)^{1/2}$, ω is the angular frequency of the a.c. signal ($\omega = 2\pi f$, where f is the linear frequency of the alternating signal). Because for a capacitor, the sinusoidal voltage

$$e=E_0\sin(\omega t+\frac{\pi}{2}) \tag{A.3}$$

where E_0 is the amplitude of the exciting signal.

So,

$$i=\frac{e}{Z} \tag{A.4}$$

$$=\frac{E_0\sin(\omega t+\frac{\pi}{2})}{R-\frac{j}{\omega C}}$$

$$=\frac{\omega CE_0}{\omega CR-j}\sin(\omega t+\frac{\pi}{2})$$

$$=\frac{\omega CE_0(\omega CR+j)}{\omega^2C^2R^2+1}\sin(\omega t+\frac{\pi}{2})$$

$$=\frac{\omega^2C^2RE_0}{\omega^2C^2R+1}\sin(\omega t+\frac{\pi}{2})+\frac{\omega CE_0}{\omega^2C^2R^2+1}\sin(\omega t+\frac{\pi}{2})j \qquad \text{(A.5)}$$

The real part of a.c. current is

$$A=\frac{\omega^2C^2RE_0}{\omega^2C^2R^2+1} \qquad \text{(A.6)}$$

and the imaginary part of the a.c. current is

$$B=\frac{\omega CE_0}{\omega^2C^2R^2+1} \qquad \text{(A.7)}$$

The ratio of the real part to the imaginary part is

$$\frac{A}{B}=\omega CR \qquad \text{(A.8)}$$

From equation (A.7),

$$R^2=\frac{\omega CE_0-B}{B\omega^2C^2} \qquad \text{(A.9)}$$

From equation (A.8),

$$R^2=\frac{A^2}{\omega C^2 B^2} \qquad \text{(A.10)}$$

From (A.9) and (A.10),

$$C=\frac{A^2+B^2}{\omega E_0 B} \qquad \text{(A.11)}$$

From (A.8) and (A.11),

$$R=\frac{AE_0}{A^2+B^2} \qquad \text{(A.12)}$$

Using a two phase lock-in amplifier, the differential capacitance can be measured for each potential applied using equation (A.11). The values of in-phase (0°) and quadrature (90°) component of a.c. response are the real and imaginary parts respectively.